plants

Article

NMR Metabolite Profiling for the Characterization of Vessalico Garlic Ecotype and Bioactivity against *Xanthomonas campestris* pv. *campestris*

Valeria Iobbi [1], Valentina Parisi [2], Anna Paola Lanteri [3], Norbert Maggi [4], Mauro Giacomini [4], Giuliana Drava [1], Giovanni Minuto [3], Andrea Minuto [3], Nunziatina De Tommasi [2,*] and Angela Bisio [1,*]

1 Department of Pharmacy, University of Genova, Viale Cembrano 4, 16148 Genova, Italy; valeria.iobbi@edu.unige.it (V.I.); giuliana.drava@unige.it (G.D.)
2 Department of Pharmacy, University of Salerno, via Giovanni Paolo II 132, 84084 Salerno, Italy; vparisi@unisa.it
3 CERSAA Centro di Sperimentazione e Assistenza Agricola, Regione Rollo 98, 17031 Albenga, Italy; anna.lanteri@rivlig.camcom.it (A.P.L.); giovanni.minuto@rivlig.camcom.it (G.M.); andrea.minuto@rivlig.camcom.it (A.M.)
4 Department of Informatics, Bioengineering, Robotics and System Science, University of Genova, via Opera Pia 13, 16145 Genova, Italy; norbert.maggi@ext.unige.it (N.M.); mauro.giacomini@unige.it (M.G.)
* Correspondence: detommasi@unisa.it (N.D.T.); angela.bisio@unige.it (A.B.); Tel.: +39-089-969754 (N.D.T.); +39-010-335-2637 (A.B.)

Abstract: The Italian garlic ecotype "Vessalico" possesses distinct characteristics compared to its French parent cultivars Messidor and Messidrôme, used for sowing, as well as other ecotypes in neighboring regions. However, due to the lack of a standardized seed supply method and cultivation protocol among farmers in the Vessalico area, a need to identify garlic products that align with the Vessalico ecotype arises. In this study, an NMR-based approach followed by multivariate analysis to analyze the chemical composition of Vessalico garlic sourced from 17 different farms, along with its two French parent cultivars, was employed. Self-organizing maps allowed to identify a homogeneous subset of representative samples of the Vessalico ecotype. Through the OPLS-DA model, the most discriminant metabolites based on values of VIP (Variable Influence on Projections) were selected. Among them, *S*-allylcysteine emerged as a potential marker for distinguishing the Vessalico garlic from the French parent cultivars by NMR screening. Additionally, to promote sustainable agricultural practices, the potential of Vessalico garlic extracts and its main components as agrochemicals against *Xanthomonas campestris* pv. *campestris*, responsible for black rot disease, was explored. The crude extract exhibited a MIC of 125 µg/mL, and allicin demonstrated the highest activity among the tested compounds (MIC value of 31.25 µg/mL).

1. Introduction

Garlic (*Allium sativum* L.) varieties, ecotype, and cultivars show a high degree of phenotypic plasticity, dependent on environmental conditions and agricultural practices [1–5]. Morphological diversity in garlic is manifested through variations in bulb size, shape, color, and clove arrangement [6,7]. Along with its morphological features, the concentrations of garlic bioactive compounds [8–11] can range significantly among different garlic varieties [12–18], leading to differences in flavor intensity and medicinal properties [19,20].

The Vessalico garlic is cultivated in northwest Italy [21,22]. The cloves of two French cultivars, Messidor and Messidrôme [23], are used every year by the Vessalico farmers for sowing. Our previous study compared Vessalico garlic with the two parent cultivars, and defined Vessalico garlic as an agricultural ecotype [22]. The conditions of growth,

harvest, and post-harvest appeared to be more important than the original genotype for the composition of garlic clove sulfur compounds [4,22,24]. Nevertheless, farmers in the Vessalico area do not all rely on the same French producers of Messidor and Messidrôme, and they do not all adopt the same agronomic practices regarding the cultivation, defense, and harvest of the product. The aim of the present study was then to identify which farms produce a garlic product different from the two French cultivars, and which can therefore be designated as true "Vessalico garlic". NMR metabolite profiling is currently used for the unbiased assessment of changes in the presence and relative abundance of small molecules in response to genetic and/or environmental factors [25,26]. In our study, a harvesting campaign involving the main seventeen farms that produce Vessalico garlic, located in the area of production of this ecotype, was performed, and NMR spectroscopy combined with multivariate data analysis were used to characterize the Vessalico garlic metabolites [27–29] and select a representative compound as a potential chemical marker to identify the Vessalico garlic from the two French parent cultivars.

In recent years, the use of natural products in sustainable agriculture has gained considerable attention to reduce reliance on synthetic inputs and promote environmentally friendly farming practices [30,31]. Natural products offer a range of benefits for crop production while minimizing adverse impacts on the ecosystem [32,33]. *Xanthomonas campestris* pv. *campestris* (Pam.) Dowson (*Xcc*) is one of the most widespread members of the *Xanthomonas* group of phytopathogens. This Gram-negative bacterium causes a devastating plant disease known as black rot and it represents a serious problem in agricultural production of *Brassicaceae* plants worldwide [34]. Black rot is a systemic vascular disease and the seedborne infection may kill young plants in the seedbed [34–37]. At present, the existing methods for *X. campestris* control rely on the use of pathogen-free seeds obtained following elimination of infection arising from seeds; however, no treatment has proven to be entirely foolproof [38]. Previous studies have reported the use of plant natural compounds, essential oils, and extracts active on *X. campestris* pv. *campestris* [39–42]. Garlic extract has been indicated as a valuable resource for organic agriculture owing to its numerous benefits in pest and disease management, soil enrichment, and plant growth promotion [43]. It has been used also for bactericidal and fungicidal activity [24,44,45]. Moreover, garlic extract is currently recognized as an active substance authorized for all purposes for use in organic farming and included in European regulations [46–50]. Thereby, to find new possibilities for the use of the garlic production waste and residues from the sales of marketed bulbs, Vessalico garlic extract was investigated as a possible agrochemical acting against *X. campestris* pv. *Campestris*.

2. Results

2.1. ^{1}H-NMR Compound Identification

The ^{1}H-NMR spectrum of a representative garlic accession (accession 12, Table S1, Supplementary Materials) is reported in Figure 1, containing as insets the high field and downfield regions (A, B, C, D). The spectral resonances were assigned based on the Chenomx 600 MHz library (CL) and custom library (CCL). A combination of NMR spectra (Figures S1–S4, Supplementary Materials), along with comparison with the published data (Table S2, Supplementary Materials), were then used to confirm metabolite identification. The spectrum showed signals belonging to carbohydrates, organic acids, amino acids, organosulfur compounds, and other metabolites (Table S2, Supplementary Materials). The high field region from 0.50 ppm to 3.50 ppm showed a signal arising from aliphatic groups of amino acids (leucine, isoleucine, valine, threonine, alanine, lysine, homoserine, glutamine, glutamate, aspartic acid, asparagine, arginine), organic acids (acetic, pyruvic, succinic, and citric), and other metabolites (acetamide, succinylacetone, riboflavin, choline). The singlets at δ_H 2.17 and 2.83 were selected as characteristic of *S*-methyl-L-cysteine and methiin, respectively. The middle field region (δ_H 3.50–5.60) showed a signal arising from the carbohydrates (fructose, xylose, α-glucose, and sucrose), sometimes strongly overlapping with the amino acid peaks (cystine, proline, glycine, methionine,

serine, pyroglutamate), the organic acids derived from carbohydrates (gluconic and lactic acid), and the methyl moiety of trigonelline. The signals, owing to the anomeric protons of sugars, were clearly visible. The downfield region exhibited the weakest signals, arising from fumaric acid, aromatic resonances of amino acids (phenylalanine), and heterocyclic compounds (histidine, trigonelline). Allyl groups of organosulfur compounds (*S*-allyl-L-cysteine, L-alliin, allicin) were also shown in this region. The following components have been described as characteristic of garlic thermal processing: pyroglutamic acid, acetic acid, and succinic acid, and their presence could be related to sample preparation [51].
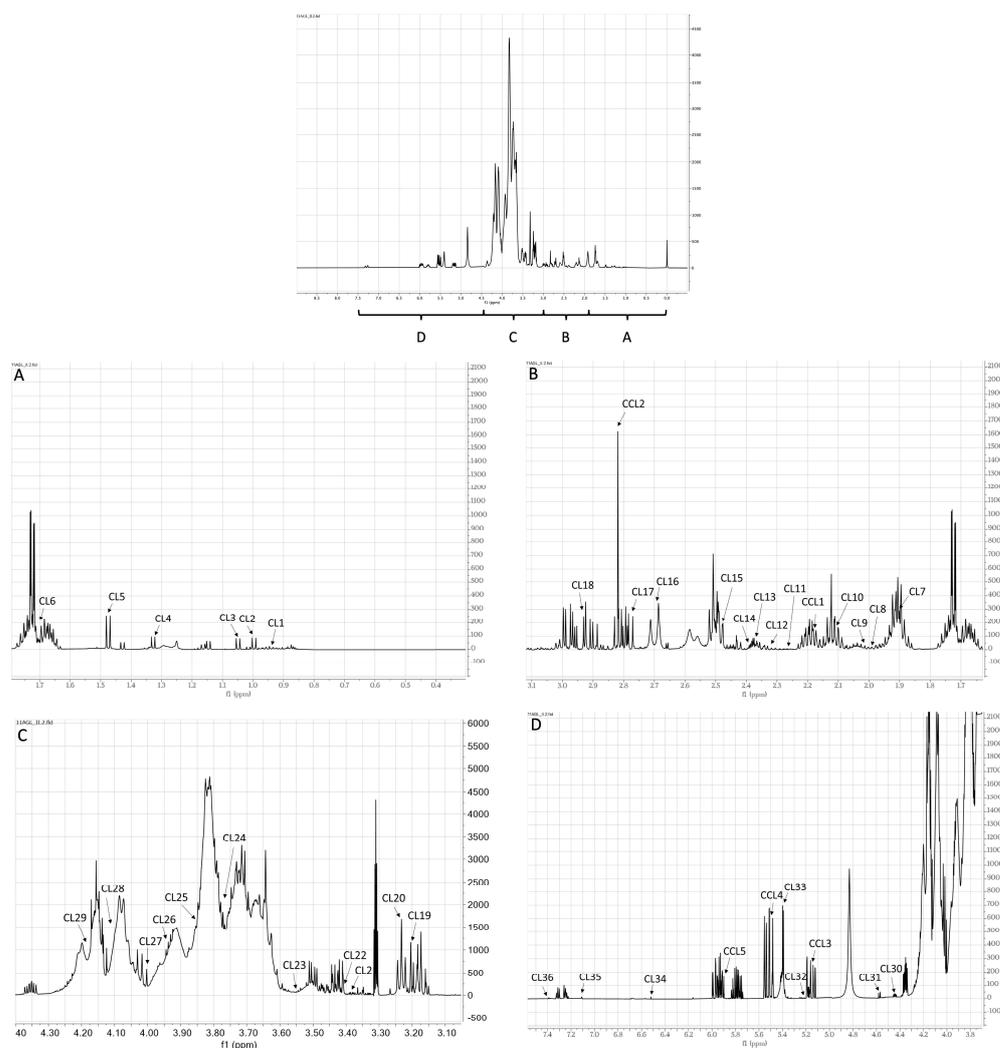
Figure 1. Representative ^{1}H-NMR spectrum of the Vessalico garlic (accession 12, Table S1, Supplementary Materials) in CD$_3$OD-KH$_2$PO$_4$ in D$_2$O at pH 6.0, 600 MHz. The spectrum was scaled to internal 1 mM deuterated sodium 3-(trimethylsilyl)-1-propionic acid (TSP), assumed to resonate at 0.00 ppm. The region δ$_H$ 0.0–7.5 was expanded in (**A**), (**B**), (**C**) and (**D**), respectively. Identified resonances are labeled according to Table S2 (Supplementary Materials): CCL1: *S*-methyl-L-cysteine, CCL2: methiin, CCL3: *S*-allyl-L-cysteine, CCL4: L-alliin, CCL5: allicin, CL1: leucine, CL2: isoleucine, CL3: valine, CL4: threonine, CL6: alanine, CL5: lysine, CL7: acetic acid, CL8: acetamide, CL9: homoserine, CL10: glutamine, CL11: succinylacetone, CL12: glutamic acid, CL13: pyruvic acid, CL14: succinic acid, CL15: riboflavin, CL16: citric acid, CL17: aspartic acid, CL18: asparagine, CL19: choline, CL20: arginine, CL21: cystine, CL22: proline, CL23: glycine, CL24: gluconic acid, CL25: methionine, CL26: serine, CL27: fructose; CL28: lactic acid, CL29: pyroglutamic acid, CL30: trigonelline, CL31: xylose, CL32: α-glucose, CL33: sucrose, CL34: fumaric acid, CL35: histidine, CL36: phenylalanine.

2.2. Multivariate Data Analysis

The spectral data (Figure S5, Supplementary Materials) matrices of garlic accessions produced by seventeen farms from the same geographical area (Vessalico, Valle Arroscia, Imperia, Italy) as well as from the French cultivars of Messidrôme and Messidor were considered. Exploratory multivariate analysis by Principal Component Analysis (PCA) allowed to visualize the complex data structure in a few dimensions: the first four components explained 91.9% of the data variance. The secondary metabolites were found to be the variables with the maximum loadings. When considering the first two Principal Components, the samples of Vessalico, Messidor, and Messidrôme appeared dispersed and overlapped: three groups of significantly correlated variables were detected (Figure S6, Supplementary Materials). However, the biplot on the second and fourth Principal Components showed a better separation between Vessalico and French samples (Figure 2), with Vessalico samples characterized, for example, by low content of methiin (CCL2) and high content of *S*-methyl-L-cysteine (CCL1), *S*-allyl-L-cysteine (CCL3), and allicin (CCL5). Only the Messidor samples appeared to be similar to the Vessalico accessions. A certain separation among the different production locations and farms was also observed (Figure S7, Supplementary Materials).
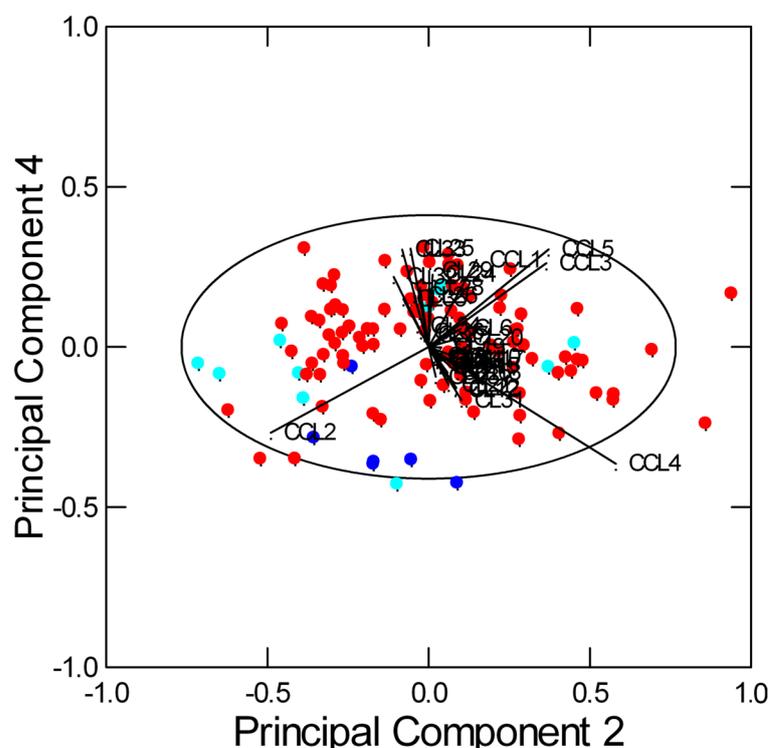
Figure 2. Results of PCA. The biplot shows the scores of the 120 spectra and the loadings of the 41 variables (5 CCL and 36 CL metabolites, Chenomx 600 MHz library and custom library metabolites) on Principal Components 2 and 4 (explaining 27.8% and 8.0% of the total variance, respectively): • Vessalico; • Messidor; • Messidrôme. The ellipse represents the 95% confidence interval.

Data analysis by means of SOMs was then performed. The number of clusters was assessed based on k-means algorithm joined to the Davies–Bouldin index (DBI) [52]. The index allows to identify the most reliable number of clusters that corresponds to a minimum value of DBI. SOMs related to CL and CCL metabolites reported two clusters (orange and green) which included only Vessalico accessions. The dark blue cluster showed that two French accession samples were mostly distributed toward the top part of the map. Moreover, some Vessalico samples exhibited several replicates in the orange cluster (e.g., 11, 12, 14), suggesting the possibility to find a homogeneous Vessalico product (Figure S8, Supplementary Materials). The PC projection showed a certain separation of Vessalico

samples from the French ones (Figure S9, Supplementary Materials). Methiin (CCL2) and L-alliin (CCL4) were the most abundant organosulfur compounds, and gluconic acid (CL24), methionine (CL25), serine (CL26), lactic acid (CL28), and pyroglutamic acid (CL29), followed by fructose (CL27) and sucrose (CL33), were the prevalent compounds among the other metabolites (Figure S10, Supplementary Materials).

Following these findings, the data analysis was repeated, with the CL and CCL metabolites being considered separately, with the aim to better investigate the Vessalico ecotype. This approach could provide more information in the search for a Vessalico biomarker.

SOMs results relative to the CL metabolites showed three clusters containing only Vessalico garlic (pale yellow, yellow, green). No cluster was represented by only French accessions (Figure S11, Supplementary Materials). Nevertheless, the PC projection showed no significative distance of Vessalico accessions from the French ones (Figure S12, Supplementary Materials). No significant differences among the relative content of CL compounds were shown by the U-matrix, unless gluconic acid (CL24), methionine (CL25), serine (CL26), lactic acid (CL28), and pyroglutamic acid (CL29), followed by fructose (CL27) and sucrose (CL33), were the most representative in all the neurons. Trigonelline (CL30) was present in very low amounts (Figure S13, Supplementary Materials). Based on these results, primary metabolites appeared not to be crucial to select a farm producing a homogeneous "Vessalico garlic".

SOMs related to CCL metabolites showed that the neurons were not specially characterized by the relative high content of certain compounds. Among the seven clusters reported as the best number of clusters (Figure 3A), the map clusterization results allowed to define two clusters of the Vessalico ecotype. The blue and orange clusters (in the left part of the map) were characterized by the sole presence of the selected ecotype with no inclusion of any French samples. The yellow cluster was occupied by the French cultivars, confirming their similarity. The top-right part of the map (green and dark green clusters) was predominantly occupied by Vessalico accessions with three samples of Messidrôme accession (19). Accession 18 (Messidor) was in the purple and light blue clusters on the right part of the map. It exhibited great similarity with respect to various Vessalico accessions (Figure 3B).
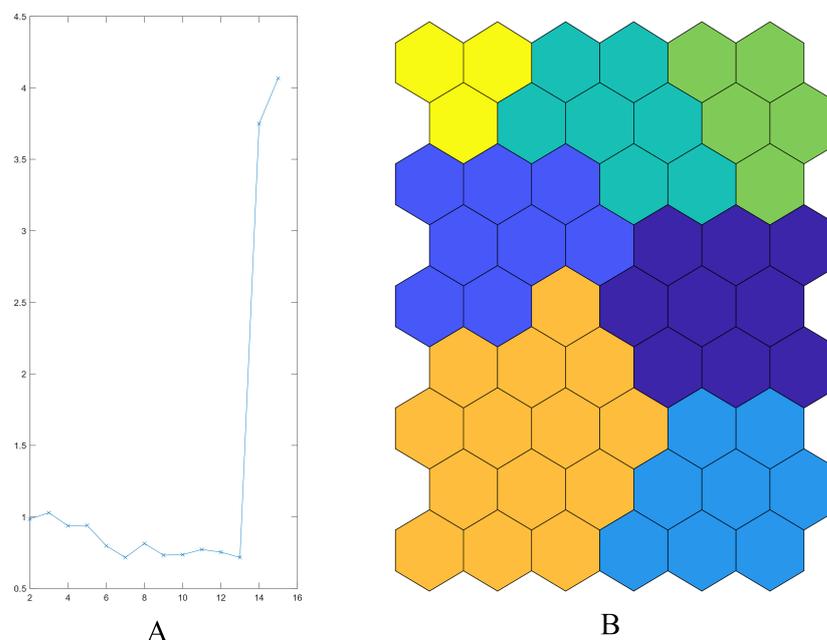
Figure 3. SOM: map clusterization. Five CCL variables (Chenomx 600 MHz custom library metabolites). (**A**) Davies–Bouldine index progression: minimum value fits the best number of clusters; (**B**) Seven clusters.

The PC projection confirmed these observations, showing a clear separation between Vessalico accessions and French cultivars (Figure 4A,B). The only Vessalico accession included in the same cluster as French cultivars was the number 12 (Figure 3B). All the replicates of this accessions were found in the orange cluster reported in Figure 4C, bordering only with samples from the Vessalico region, and no French accession. These results allowed us to assume that the product of farm 12 was the only homogeneous product of Vessalico garlic. Farm 14 was represented by five samples in the orange cluster with one outlier. Farm 11 was characterized by three samples in the orange cluster and three in the blue one. A relatively higher content of methiin (CCL2) and L-alliin (CCL4) could be attributed to Vessalico accessions of the orange cluster, although no significant differences were observed (Figures 4C and 5).
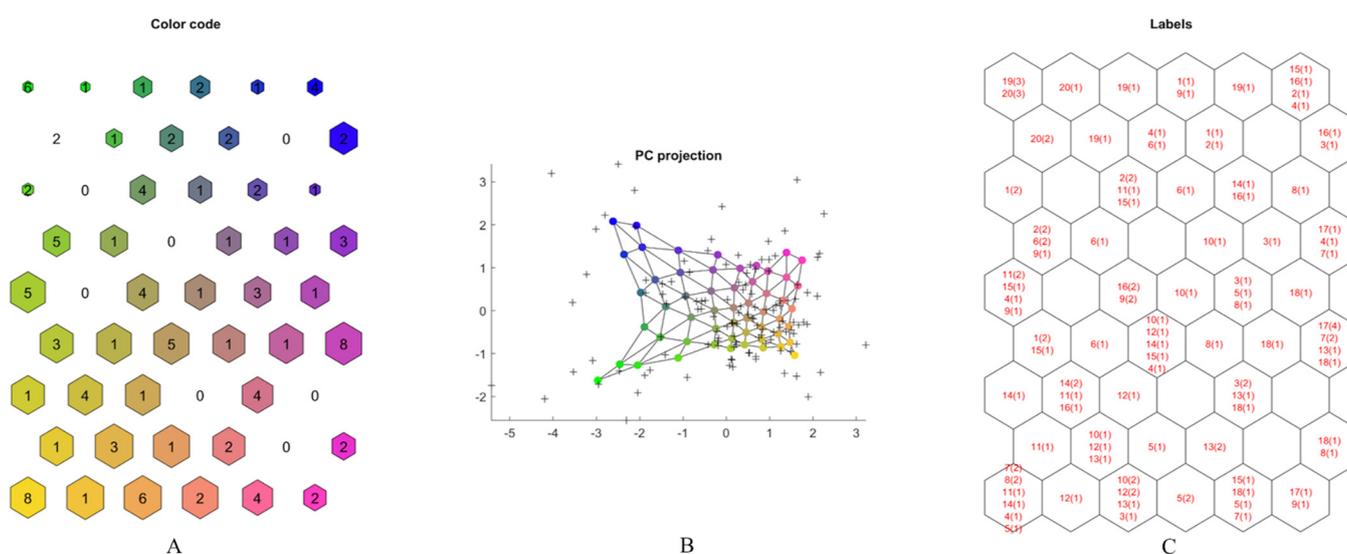
Figure 4. SOM: graphical representation of five CCL variables (Chenomx 600 MHz custom library metabolites) on map. (**A**) SOM output map with color code association. Similar colors have similar characteristics; numbers correspond to hit numbers. The dimensions of the hexagons are related to the distance between neurons (the greater the size, the greater the distance). (**B**) Principal component projection of the map; (**C**) labelled SOM output map, for each neuron the corresponding accession number (Table S1, Supplementary Materials) and number of replicates (in parentheses) are shown.

An Orthogonal Partial Least Squares Discriminant Analysis (OPLS-DA) was applied to a reduced data matrix containing only the typical Vessalico accessions, as obtained from SOM analysis (accessions 11, 12, 14), together with the French accessions (accessions 18, 19, 20). This reduced two-class data matrix contained 18 spectra belonging to each of the two categories (Vessalico and France). An OPLS-DA model with two components was computed and validated, with $R^2(Y) = 0.859$ and $Q^2(Y) = 0.764$. This model allowed to discriminate between the Vessalico ecotype and the French varieties (Figure 6), showing high selectivity and specificity as confirmed by the misclassification matrix (94% of correct classifications; 89% of correct predictions).

The OPLS-DA method was also used to select the most discriminant metabolites based on values of VIP (Variable Influence on Projections) greater than 1. VIP variables for this set of data are shown in Figure 7.
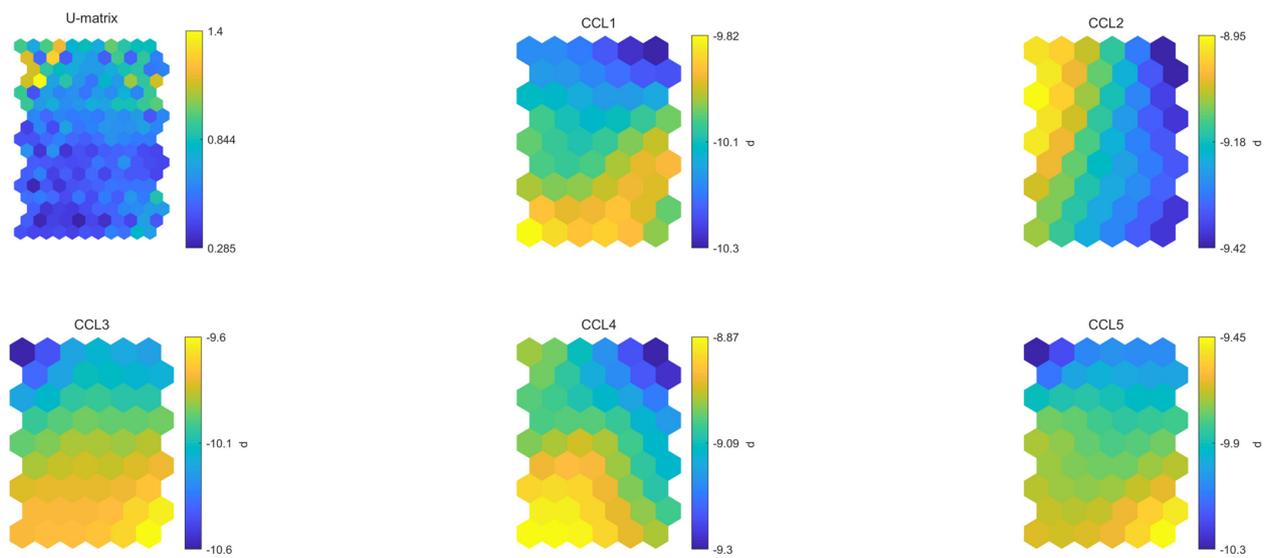
Figure 5. SOM: U-matrix and maps for each CCL variable (Chenomx 600 MHz custom library metabolites). Similar color gradations indicate highly correlated variables. CCL1: *S*-methyl-L-cysteine, CCL2: methiin, CCL3: *S*-allyl-L-cysteine, CCL4: L-alliin, CCL5: allicin.
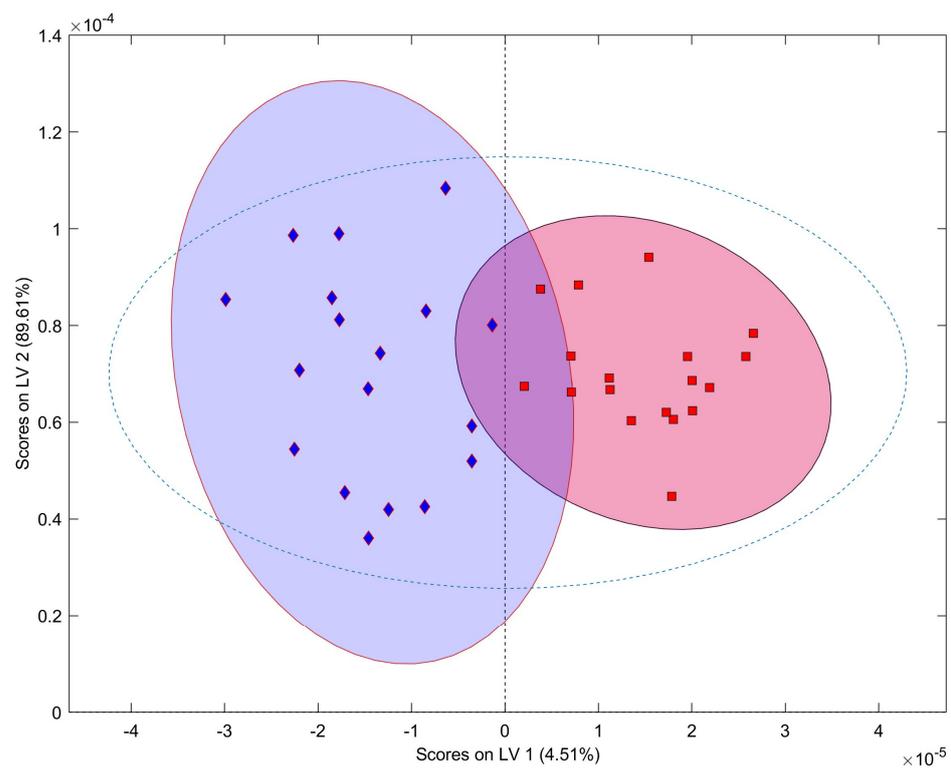
Figure 6. OPLS-DA score plot with confidence ellipses for the two classes: Vessalico (red square) and France (blue diamond).
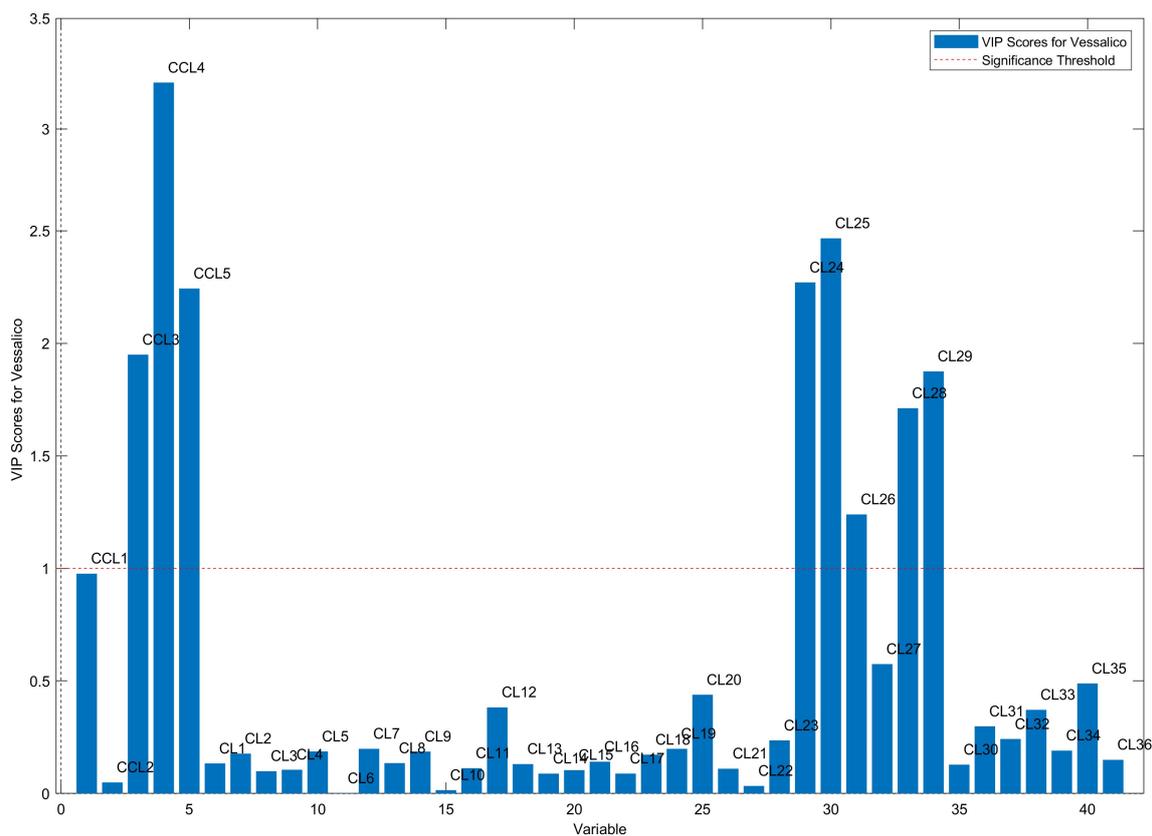
Figure 7. VIP (Variable Influence on Projections) values: the most discriminant variables (VIP > 1) are CCL3 (*S*-allyl-L-cysteine), CCL4 (L-alliin), CCL5 (allicin), CL24 (gluconic acid), CL25 (methionine), CL26 (serine), CL28 (lactic acid), and CL29 (pyroglutamic acid).

ANOVA confirmed that all variables having VIP > 1 were significantly different ($p < 0.001$) between the selected Vessalico garlic and French cultivars.

Finally, the model was implemented to predict the class of the remaining 84 samples from Vessalico, not used for the computation of the model. Despite the small number of samples in the training set with respect to the large number of test samples, the model showed good performance, accepting 55% of the Vessalico samples.

2.3. *S-Allyl-L-Cysteine Quantification*

Among the most discriminant variables, sulfur compounds, which are mainly responsible for the garlic aroma, were considered to find a simple way to distinguish between the accession identified as representative of the Vessalico garlic (accession 12) and that identified as representative of the two French parent cultivars. *S*-allyl-L-cysteine was selected to be quantified in the three extracts due to its stability compared to L-alliin and allicin, and because it had an easily identifiable multiplet at 5.81 ppm (Figure 8). The quantification of *S*-allyl-L-cysteine in the garlic extract was carried out through qNMR using a 1D-NOESY sequence. Results showed that the *S*-allyl-L-cysteine content was 135.67 ± 2.18 µg/g in fresh Vessalico garlic cloves, while it was present in negligible amounts in the parent cultivars Messidor and Messidrôme.
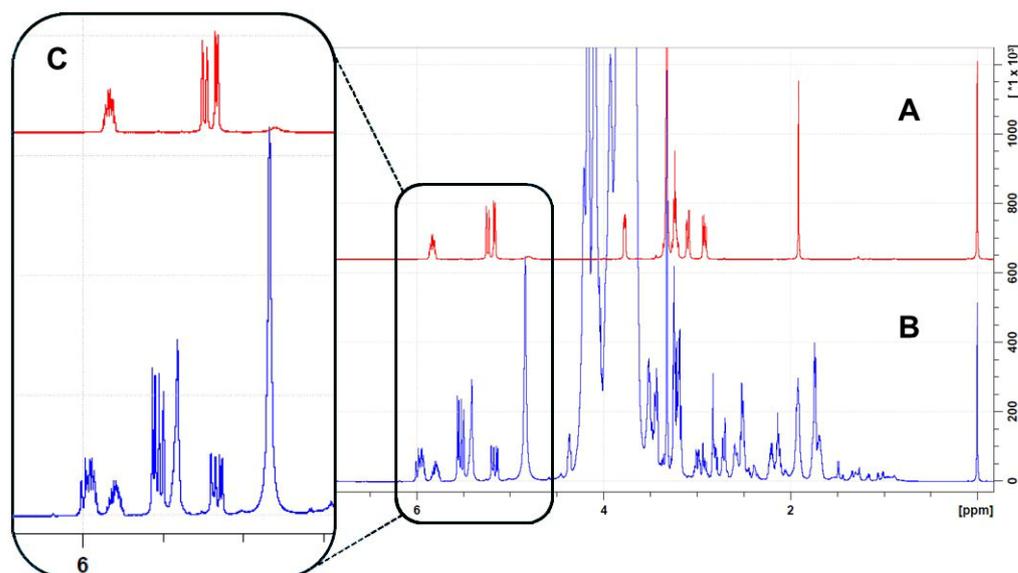
Figure 8. Spectra (¹H NMR) of *S*-allyl-L-cysteine (**A**), and accession 12 extract (**B**). Zoom of spectra from δ_H 4.70 ppm to 6.30 ppm (**C**). The isolated doublet at 5.18 ppm (in the black square) of *S*-allyl-L-cysteine was used for the quantification.

2.4. Antibacterial Activity

The minimum bacterial concentrations (MICs) of the extract of accession 12 was determined against two strains of *Xanthomonas campestris* pv. *campestris* by using the diluting broth technique. Pure sulfur compounds (S-allyl-L-cysteine, S-methyl-L-cysteine, L-alliin, allicin, and methiin) were also tested. Ampicillin and streptomycin sulphate were included in the test as references for their activity on Gram-negative bacteria [53–58]. Allicin proved to be the most active substance against both *X. campestris* pv. *campestris* strains, with a MIC value of 31.25 μg/mL (Table 1). The crude extract was characterized by a MIC value of 125 μg/mL, while S-allyl-L-cysteine, S-methyl-L-cysteine, L-alliin, and methiin showed a MIC of 500 μg/mL against both strains. Ampicillin showed a MIC of 0.25 μg/mL against strain 1 and a MIC value of 0.5 μg/mL against strain 2. Streptomycin sulphate showed a value of MIC of 0.5 μg/mL against strain 1 and a MIC value of 1 μg/mL against strain 2. The growth of *X. campestris* pv. *campestris* was visible in drug-free wells (control of growth) and no growth was observed in wells containing non-inoculated sterile Mueller Hinton Broth (MHB) medium as a blank control.

Table 1. Evaluation of the MICs of extract, pure compounds, and antibiotics against *Xanthomonas campestris* pv. *campestris*.

Treatment	MIC			
	(μg/mL)		μM	
	Strain 1	Strain 2	Strain 1	Strain 2
S-allyl-L-cysteine	500	500	3101.3	3101.3
S-methyl-L-cysteine	500	500	3698.77	3698.77
L-alliin	500	500	2821.35	2821.35
Methiin	500	500	3307.10	3307.10
Allicin	31.25	31.25	192.57	192.57
Crude extract	125	125	-	-
Ampicillin	0.25	0.5	0.72	1.43
Streptomycin sulphate	0.5	1	0.34	0.69

3. Discussion

In this study, an NMR metabolite profiling technique was applied as a first approach to identify which farm, among the main producers of garlic in the Vessalico area, produced a product that could be referred to as true "Vessalico garlic" that differs and can be distinguished from the two French cultivars used for sowing. The main metabolites of garlic include primary metabolites, such as amino acids and carbohydrates, as well as secondary metabolites, such as organosulfur compounds, and more polar compounds of phenolic and steroidal origin, often glycosylated [8,9,11,59]. Organosulfur compounds in intact garlic cloves include about equal amounts of γ-glutamyl-peptides and *S*-alk(en)yl-L-cysteine sulfoxides (ACSOs) [which include (+)-*S*-allyl-L-cysteine sulfoxide (L-alliin), (+)-*S*-(trans-1-propenyl)-L-cysteine sulfoxide (isoalliin), (+)-*S*-methyl-L-cysteine sulfoxide (methiin), and (1*S*,3*R*,5*S*)-3-carboxy-5-methyl-1,4-thiazane-1-oxide (cycloalliin)]. Intermediate compounds in the biosynthesis of ACSOs from γ-glutamyl peptides are *S*-alk(en)yl-cysteines such as (+)-*S*-allyl-L-cysteine (SAC), (+)-*S*-(trans-1-propenyl)-L-cysteine (SPC), and (+)-*S*-methyl-L-cysteine (SMC). Alkyl alkanethiosulfinates such as *S*-allyl cysteine sulfoxide (allyl 2-propenethiosulfinate, allicin) and others are formed from the two main classes of secondary metabolites through enzyme reactions when the raw garlic is cut or crushed [4,9,60]. In our work, we selected five sulfur compounds that could be connected to the various conditions in which garlic bulbs can be found after harvesting and storage [61,62]. Upon crushing the garlic, Allicin abundance has been shown to amount to 60–90% of the total thiosulfinates [11]. The relative content of *S*-alk(en)yl-L-cysteine sulfoxides (L-alliin and methiin) in garlic is known to be affected by several genetic and environmental factors (e.g., climatic conditions, soil composition, irrigation, fertilization, harvest date, etc.) [63]. The concentration of *S*-methyl-L-cysteine and *S*-allyl-L-cysteine is higher in aged garlic [64].

The preliminary findings obtained through explorative analysis by PCA did not highlight a clear separation between the Vessalico garlic and the French varieties. The results obtained by SOM on the profile of the only CL metabolites did not allow the identification of a homogeneous Vessalico product by cluster distribution. However, SOMs performed on the secondary metabolite data enabled the identification of a homogeneous product belonging only to one cluster which was different from the parent cultivars: that product was identified as true "Vessalico garlic".

When the spectral data were submitted to supervised multivariate analysis by OPLS-DA, a reliable class model was computed, allowing to highlight the high influence of the variables able to discriminate between the Vessalico garlic and the parent French varieties. According to VIP values, eight representative indicators were identified as characteristic of the Vessalico garlic. The indicators included three sulfur compounds, amino acids, and organic acids: *S*-allyl-L-cysteine (SAC), (±)-*S*-allyl-L-cysteine sulfoxide (L-alliin), allyl 2-propenethiosulfinate (allicin), methionine [65], serine [65], lactic acid (characteristic of raw garlic [51]), gluconic acid [66,67], and pyroglutamic acid [51,68], produced by Maillard reactions and characteristic of aged garlic or produced after thermal processing [51]. The largest VIP value was shown by (±)-*S*-allyl-L-cysteine sulfoxide (L-alliin), which is generally considered to be a major factor in determining the quality of garlic [69]. The harvest of garlic is conducted once a year. The garlic is then stored for up to 12 months before being sold or consumed, and the content of sulfur compounds may vary considerably depending on the period and method of storage [24,64]. L-alliin is a thermolabile compound [70] because of its unstable sulfoxide bond. The literature data about changes in the relative amount of L-alliin at different processing stages of cultivation and storage are variable [24,69,71]. Nonetheless, it is described as one of the most degraded compounds due to prolonged storage [62]. Allicin, one the most important biologically active compounds found in crushed or homogenized garlic, is extremely unstable due to the presence of a thiol group [72,73], and its half-life varies depending on the concentration and temperature of the storage solvent [74]. *S*-allyl-L-cysteine is a very stable compound [75], its content increasing during storage [62], as a result of the hydrolysis of γ-glutamyl-*S*-allyl-L-cysteine (GSAC) by the γ-glutamyl transferase enzyme (γ-GTP, EC 2.3.2.2) [75],

and unaffected during fermentation and packing steps, similarly to other organosulfur compounds [62]. Thus, *S*-allyl-L-cysteine was selected as a representative metabolite. This metabolite contributes heavily to the health benefits of garlic and it is well-documented for its antioxidant, anti-apoptotic, anti-inflammatory, anti-obesity, cardioprotective, neuroprotective, and hepato-protective properties [76]. *S*-allyl-L-cysteine content in intact garlic is in the range of 19.0–1736.3 μg/g (fresh weight) [75,77,78]. The concentration of *S*-allyl-L-cysteine increases during storage at room temperature (950.0 μg/g) [62], and the content in processed garlic, such as frozen and thawed garlic, pickled garlic, fermented garlic extract, and black garlic is even higher, reaching values of 8021.2 μg/g [78–80]. In the present study, the content of *S*-allyl-L-cysteine in the fresh cloves of the garlic accession selected as representative of the Vessalico garlic was 135.67 ± 2.18 μg/g. Since the content of this compound was almost undetectable in the French parent cultivars, *S*-allyl-L-cysteine could be considered a possible chemical marker to distinguish the Vessalico ecotype from the two French accessions.

Although NMR metabolite profiling is currently considered a reliable approach for the assessment of presence and relative abundance of small molecules [27,29,81,82], genetic information is, at present, the only method that provides a final validation with respect to the description of plant ecotypes [83–86]. Further studies will be needed to explore genetic information, thus providing a more comprehensive characterization of the Vessalico ecotype.

Agroecological pest management [87] is becoming increasingly important as part of a sustainable agriculture vision that incorporates various approaches and areas [30]. The EU bactericides are restricted to a few agents, and non-bactericidal antibiotics are no longer approved [88,89]. In this scenario, the use of plant extracts as antimicrobials is becoming more crucial [90]. Garlic and its bioactive components are well-known for their antimicrobial activity against phytopathogens [45,91], giving rise to the idea of a possible application in biological and integrated pest management. Currently, there is no treatment for the control of black rot caused by *X. campestris*. Consequently, the research of natural products and plant extracts may identify new antimicrobial agents to control this bacterial disease. *X. campestris* pv. *campestris* is the causal agent of black rot of brassicas and is currently a significant problem affecting a large group of horticultural crops grown in the open field. As previously mentioned, its primary spread occurs through the seed, but there are currently no tanning agents available to address this type of problem. Furthermore, in the field, it used to be contained with the use of copper [92] which is undergoing strong regulation [93]. Previously, the use of copper was coupled with the use of dithiocarbamates [94], whose usage is currently no longer allowed in the EU. Some brassicaceous species are also included in the "baby leaf" category for which the use of synthetic products presents strong limitations due to the application of very low residual limits. "Baby leaves" are also one of the crops of choice in "vertical farming", an emerging growing practice [95]. This type of cultivation involves the exploitation of a confined environment where irrigation water is continuously reused. The environment, therefore, is particularly conducive to bacterial diseases and not very suitable for the application of copper-based compounds often characterized by a marked phytotoxic effect. The present study investigated the antimicrobial activity of garlic extract against *X. campestris* pv. *campestris.* Other plant extracts have been tested against *X. campestris* pv. *campestris*, with MIC values ranging from 0.15 mg/mL to 1.25 mg/mL [96–98]. In this study, the MIC of garlic extracts against *X. campestris* pv. *campestris* was 125 μg/mL, thus showing a good activity compared to other extracts discussed in the literature. Allicin is recognized as the main compound responsible for the antimicrobial activity of garlic [99–101], and its activity against *X. campestris* pv. *malvacearum* [102] and *X. campestris* pv. *campestris* [45] (Zone of Inhibition Test) has been explored. The MIC of allicin against *X. campestris* pv. *campestris* has been shown to be lower than that of commercial copper-based products against *X. campestris* [103,104] and lower than that of other natural products against *X. campestris* pv. *vesicatoria* (geraniol, MIC = 250 μg/mL; thymol, MIC = 125 μg/mL; o-vanillin, MIC = 250 μg/mL) [105].

4. Materials and Methods

4.1. General Experimental Procedures

Ultra-pure water and all organic solvents of analytical grade were purchased from ROMIL-UpSTM (Waterbeach, Cambridge, UK). Deuterium oxide (D2O, 99.90% D), CD_3OD (99.95% D), and 3-(trimethylsilyl) propionic-2,2,3,3-d 4 acid sodium salt (TSP) were purchased from the Sigma-Aldrich chemical company (Sigma-Aldrich, Milano, Italy). The standard compounds chosen as representatives of their main class were *S*-allyl-L-cysteine, *S*-methyl-L-cysteine, and ($\pm$)-L-alliin $\geq$ 90%, all of which were purchased from Merck KGaA (Darmstadt, Germany), allicin, obtained from MedChemExpress (Monmouth Junction, NJ, USA), and methiin, purchased from Abcam (Cambridge, UK).

4.2. Plant Material

Seventeen accessions of *Allium sativum* ecotypes ("Vessalico garlic"), grown under field conditions in numerous farms located in six different areas of Valle Arroscia (Imperia, Italy), along with three commercial accessions of the French cultivars Messidrôme and Messidor (one of Messidrôme and two of Messidor, respectively, representing all commercial sources from which farmers acquire their supply) were collected and authenticated based on clove morphology (Table S1, Supplementary Materials). The identification of all the garlic accessions was performed by Dr. Andrea Minuto [106,107]. The vouchers of all the accessions were deposited at CERSAA (Albenga, Italy).

4.3. Sample Collection and Preparation

Harvesting took place in June 2023, when the garlic reached full ripeness, indicated by the falling of the neck or the drying of leaves. The harvested garlic was then stored at cellar temperature. The study was conducted during late autumn, replicating the conditions in which commercial garlic is typically sold throughout the autumn and winter season. A random selection of clove samples was conducted, and each individual undamaged clove was meticulously peeled, frozen, and lyophilized in a freeze-dryer (Super Modulyo, Edwards, UK) for 48 h. Three biological replicates for each accession were used, with a total of 60 samples. All samples were sealed in plastic bags and stored dry in the dark until analysis. The dried material (about 35 g per sample) was then ground.

The powder samples were prepared following the method reported by Tajidin et al. [108]. Briefly, 50 mg of each dried sample was extracted by vortexing (30 s) with 1.0 mL of CD_3OD (0.5 mL, 99.95%) and KH_2PO_4 (0.5 mL) buffer in D_2O (pH 6.0) containing 0.1% of 3-(trimethylsilyl) propionic-2,2,3,3-d_4 acid sodium salt (TSP) and then sonicated (30 min) (Branson 2510E-MTH, Bransonic®, Milano, Italy) at room temperature. The clear deuterated supernatant obtained after centrifuging (D3024 Microcentrifuge, Scilogex, Rocky Hill, CT, USA) at 13 rpm for 10 min was transferred into NMR tubes. The extracts for the NMR quantification and antimicrobial assays were prepared using 85 g of peeled and crushed cloves with 300 mL of $CH_3OH \geq$ 99.9%/H_2O 1:1 50:50 at 25 °C, then sonicated (VWR USC200TH, VWR International, Leuven, Belgium) at a fixed frequency of 37 KHz for 30 min at room temperature. The supernatant obtained was filtered and evaporated using a rotary evaporator. All the procedures were carried out in a timely manner to avoid degradation of compounds [73,109]. The extract powders were then stored in a laboratory freezer (-20 °C).

4.4. NMR Spectroscopy and Processing

NMR data were acquired on a Bruker Ascend™ 600 NMR spectrometer (Bruker BioSpin GmBH, Rheinstetten, Germany) equipped with a Bruker 5 mm TCI CryoProbe at 300 K, operating at 600 MHz, with the temperature maintained at 27 °C, and H_2O-d_2 was used as an internal lock. Each ^{1}H NMR spectrum consisted of 64 scans, 2.05 s acquisition time, a relaxation delay (RD) of 4 s, mixing time of 0.01 s, and a spectral width of 13.33 ppm (corresponding to 8000 Hz). A pre-saturation sequence (NOESY-presat sequence, Bruker: noesygppr1d) was used to suppress the residual signal of water [110–112]. A Chenomx 600 MHz custom library (CCL) (Chenomx NMR Suite 8.6, Chenomx Inc., Edmonton, AB, 252 Canada) was

set up by means of pure secondary metabolites obtained from commercial sources (Sigma-Aldrich, Milano, Italy). The Chenomx Compound Builder tool was used. The CCL included five standard compounds: *S*-methyl-L-cysteine (SMC) (CCL1), *S*-methyl-L-cysteine sulfoxide (methiin) (CCL2), *S*-allyl-L-cysteine (SAC) (CCL3), (±)-*S*-allyl-L-cysteine sulfoxide (L-alliin) (CCL4), and allyl 2-propenethiosulfinate (allicin) (CCL5). Additionally, 36 metabolites from the Chenomx 600 MHz library, selected based on literature data [28,29,51,113,114], were used (Table S2, Supplementary Materials). Each ^{1}H NMR spectrum was acquired using the 1D. All spectra were acquired in duplicates. The metabolites were identified based on the comparison of their ^{1}H NMR spectra to those of the reference compounds in both the custom and the 600 MHz version libraries (MSI level of identification according to Sumner et al.) [115].

4.5. NMR Data Analysis

NMR data were acquired on a Bruker. NMR spectra analysis and metabolite quantification were then performed by using the online server NMRProcFlow (INRA UMR 1332 BFP, Bordeaux Metabolomics Facility, Villenave d'Ornon, France) [116] following the method reported by Grimaldi et al. [117]. Briefly, corrections of phasing and baseline were performed manually for all spectra using TOPSPIN version 3.2. All spectra were calibrated by using the internal standard at 0 ppm. Spectral area integration was achieved by variable sized bucketing using the online server NMRProcFlow. Buckets with a signal-to-noise ratio above 3 were selected for further analysis. The residual solvent regions of water (δ_H 4.65–4.75) were removed (Figure S5, Supplementary Materials). The data matrices generated by NMRProcFlow, one of five buckets (CCL compounds) and one of 36 buckets (CL compounds), were then subjected to multivariate analysis. The metabolite identification was assessed by comparison of their ^{1}H NMR spectra to those of the Chenomx 600 MHz libraries.

4.6. Multivariate Data Analysis

Exploratory data analysis and an ANOVA were performed using the Systat software for Windows Version 13 (Systat Software Inc., Chicago, IL, USA). A Principal Component Analysis (PCA) was conducted on the spectral data after Pareto scaling.

Self-Organizing Maps (SOMs) were employed as an unsupervised model, utilizing Matlab R2022a (MathWorks, Inc., Natick, MA, USA) and SOM Toolbox 2.1 [118]. SOMs are characterized by their ability to organize and process information in a network-like structure. To prepare the data for analysis, a series of pre-processing steps were undertaken. First, the dataset underwent a log transformation, following the approach outlined by van den Berg et al. [119]. This transformation was necessary to mitigate the dominance of variables with higher ranges, as they could disproportionately influence the distances within the map. Additionally, a variance-based normalization technique was applied to ensure balanced representation of the variables. The SOM training process consisted of two distinct phases: the rough phase and the refinement phase. In the rough phase, the SOM was trained with a larger radius and learning rate, an approach which facilitated a more extensive exploration of the data space. This phase also took into consideration the influence of the most distant nodes, enabling a comprehensive representation of the dataset. Following the rough phase, the refinement phase commenced, employing a smaller radius and learning rate to fine-tune the SOM. This phase allowed for localized adjustments, leading to convergence towards a final map representation. Upon completion of the training process, the U-matrix was generated to visually depict the distances between neighboring map units. The U-matrix facilitated cluster identification, with uniform areas indicating distinct clusters and higher values highlighting cluster boundaries. In addition to the U-matrix, other maps were generated to represent the component plan, focusing on single compounds. Highly correlated variables exhibited similar map patterns, enabling insights into the interrelationships among the variables. Hits, defined as the number of times a map unit responded to inputs, were associated with specific units within the map. Hits served as an indicator of the amount of input information collected by each neuron, providing valuable information about the data distribution. The use of SOMs in

this study established the framework for subsequent data analysis and interpretation. The described steps ensured proper data pre-processing, effective training, and visualization of the resulting SOM representation, setting the stage for a comprehensive understanding of the underlying patterns within the dataset.

OPLS-DA [120] was used for discriminating the representative samples of the Vessalico ecotype from the French cultivars, using a MATLAB toolbox called PLS_toolbox by Eigenvector. The OPLS-DA model was validated and used to predict the class of test samples (i.e., Vessalico accessions not used for computing the OPLS-DA model). The quality of the model was evaluated in terms of R^2 and Q^2 and by means of misclassification matrices [121]. The most characterizing metabolites were selected on the basis of the Variable Influence on Projections (VIP values) of OPLS-DA.

4.7. S-Allyl-L-Cysteine Quantification

Among the characterizing metabolites, *S*-allyl-L-cysteine (CCL3) was selected as a representative metabolite, owing to the presence of an isolated doublet at 5.81 ppm, and then quantified in the Vessalico garlic (accession 12), Messidor, and Messidrôme extracts. A calibration curve of SAC was made in a concentration range of 10–500 μg/mL. The linearity of the instrumental response in the analyzed concentration range was confirmed, as inferred by the following fitting curve parameters: y = 787,835, x − 6866.9, R^2 = 0.9994. The Limit of Detection (LOD) and the Limit of Quantification (LOQ) were determined by serially diluting *S*-allyl-L-cysteine. The analysis was performed until the results of signal-to-noise ratio (S/N) reached the values of 3:1 and 10:1. The obtained values of the LOD and LOQ were 2.0 μg/mL and 8.0 μg/mL, respectively. All the data needed were exported into a spreadsheet workbook using the "qHNMR" template.

4.8. Antibacterial Activity

Two strains of *Xanthomonas campestris* pv *campestris* obtained from the microbial collection of CeRSAA were employed in this study. The strains were previously isolated from different symptomatic plant hosts (*Brassica oleracea* and *Eruca vesicaria*), identified by molecular sequencing, and characterized according to the pathogenicity test (Koch postulates confirmation) [122,123]. Sterile stock solutions in 80% dimethyl sulfoxide (DMSO) (Sigma Aldrich, St. Louis, Missouri, USA) of the extract and pure compounds (*S*-allyl-L-cysteine, *S*-methyl-L-cysteine, (±)-L-alliin, allicin, and methiin) (20 mg/mL) were prepared and stored at −20 °C. Dilutions 1:10 of the six stock solutions were obtained using Mueller Hinton Broth (Merck-Millipore, Burglinton, MA, USA). The concentration obtained (2000 μg/mL) was, on two occasions, the highest test concentration, and 100 μL of each solution was transferred in a well of the first column. Sterile stock solutions in 80% dimethyl sulfoxide (DMSO) (Sigma Aldrich, St. Louis, MO, USA) of ampicillin (Sigma-Aldrich, Milano, Italy) and streptomycin sulphate (VWR Life Science, Radnor, PA, USA) (0.64 mg/mL) were prepared and stored at −20 °C. Dilutions 1:10 of the two antibiotics were obtained using Mueller Hinton Broth. The concentration obtained (64 μg/mL) was, on two occasions, the highest test concentration, and 100 μL of each solution was transferred in a well of the first column. One-day-old bacteria cultures were diluted in Buffered Peptone Water (VWR Life Science, Radnor, PA, USA) to obtain a bacterial suspension acclimated to 0.5 on the McFarland scale. Microbial inoculums were then diluted to 1/150 in Mueller Hinton Broth (Merck-Millipore, Burglinton, MA, USA) to obtain a final concentration of approximately 5×10^5 cells/mL. The MICs of extracts and pure compounds of *S*-allyl-L-cysteine, *S*-methyl-L-cysteine, (±)-L-alliin, allicin, and methiin were determined by following the microdilution procedure [124] reported by the Clinical and Laboratory Standards Institute [125] using Mueller Hinton Broth as the test medium. Briefly, 50 μL of inoculum obtained as described above was added to equivalent volumes of various concentrations of extracts and pure compounds of *S*-allyl-L-cysteine, *S*-methyl-L-cysteine, (±)-L-alliin, allicin, and methiin, distributed across a 96-well microplate, and prepared from two-fold serial dilutions ranging from 0.977 μg/mL to 1000 μg/mL. Simultaneously, the inoculum was

added to equivalent volumes of ampicillin and streptomycin sulphate distributed across a 96-well microplate and prepared from two-fold serial dilutions ranging from 0.031 μg/mL to 32 μg/mL. The activity of DMSO as a negative control was tested in the last row and it ranged from 0.039 μL/m to 40 μL/mL. The last line contained five drug-free wells control of growth, and three wells containing non-inoculated sterile Mueller Hinton Broth (MHB) medium as a blank control. To avoid degradation of the compounds [73,109], all procedures were executed in a timely manner, and the microplate and solutions were kept on ice during all the working procedures until the following incubation step. After 24 h of incubation in dark conditions at 35 °C, the lowest concentration of compounds preventing visible growth was recorded as the MIC. All MICs were obtained in triplicates.

5. Conclusions

In conclusion, the comparative characterization of the Vessalico garlic, along with the French cultivars Messidor and Messidrôme, offers a unique opportunity to explore the intricate relationships between garlic ecotypes and their distinct regional adaptations. The findings of this study hold significant implications for agricultural practices, culinary traditions, and the preservation of cultural heritage, ultimately guiding future conservation efforts and sustainable cultivation practices for these valuable garlic varieties. The NMR metabolomic study, followed by multivariate data analysis, allowed to define the secondary metabolites more related to the area and to the methods of cultivation and harvesting. Moreover, accession 12 was identified as the only product of Vessalico different from the two French parent cultivars. Among the secondary metabolites, *S*-allyl-L-cysteine could be considered as the biomarker to identify the Vessalico garlic among the other French parent cultivars. Future research to obtain genetic data, thereby offering a more comprehensive characterization of the selected ecotype, will be performed.

Although the antimicrobial activity of garlic extracts and allicin is widely documented in the literature [45,126,127], no study on the evaluation of the MICs of pure compounds of *S*-allyl-L-cysteine, S-methyl-L-cysteine, (±)-L-alliin, allicin, and methiin against *X. campestris* pv. *campestris* through the dilution broth technique has been conducted so far. The formation of allicin, the most active substance against *X. campestris* pv. *campestris*, when alliinase cleaves alliin after the cell breaks, is the basis of its specific role in plant defense mechanisms [128]. Given the impossibility of applying antibiotics and synthetic products, as well as the progressive reduction of the legal limits allowed for copper-based products and considering the low environmental impact of plant extracts and pure compounds, the potential use of garlic extracts as well as allicin (in appropriate formulations to avoid its degradation) in the control of infections caused by *X. campestris* pv. *campestris* is currently of great interest and relevance. Our results suggest that garlic extracts could be considered to control the bacterial disease caused by *X. campestris* pv. *campestris*. Nonetheless, further studies in vivo on formulation and protection strategies are needed for use in conventional and organic agriculture.

Supplementary Materials: The following supporting information can be downloaded at: https://www.mdpi.com/article/10.3390/plants13091170/s1, Figure S1: Representative 1H-NMR spectrum of Vessalico garlic; Figure S2: Representative HSQC spectrum of Vessalico garlic; Figure S3: Representative HMBC spectrum of Vessalico garlic; Figure S4: Representative COSY spectrum of Vessalico garlic; Figure S5: 1H-NMR spectra of garlic accessions; Figure S6. Results of PCA. CL and CCL variables; Figure S7: Results of PCA applied to garlic accessions from different locations and farms; Figure S8: Results of SOMs. Map clusterization for CL and CCL variables; Figure S9: Results of SOMs. Graphical representation of map for CL and CCL variables; Figure S10: Results of SOMs. U-matrix and maps for each CL and CCL variables; Figure S11: Results of SOMs. Map clusterization for CL variables; Figure S12: Results of SOMs. Graphical representation of map for CL variables; Figure S13: Results of SOMs. U-matrix and maps for each CL variable; Table S1: List of garlic accessions used in the study; Table S2: 1H NMR chemical shifts (δ) and coupling constants (Hz) of Chenomx 600 MHz library (CL) and custom library (CCL) metabolites. (See Refs. [28,29,51,81,114,115,129–147]).

References

1. Casals, J.; Rivera, A.; Campo, S.; Aymerich, E.; Isern, H.; Fenero, D.; Garriga, A.; Palou, A.; Monfort, A.; Howad, W.; et al. Phenotypic diversity and distinctiveness of the Belltall garlic landrace. *Front. Plant Sci.* **2023**, *13*, 1004069. [CrossRef] [PubMed]
2. Egea, L.A.; Mérida-García, R.; Kilian, A.; Hernandez, P.; Dorado, G. Assessment of genetic diversity and structure of large garlic (*Allium sativum*) germplasm bank, by diversity arrays technology "genotyping-by-sequencing" platform (DArTseq). *Front. Genet.* **2017**, *8*, 98. [CrossRef] [PubMed]
3. Volk, G.M.; Henk, A.D.; Richards, C.M. Genetic diversity among U.S. garlic clones as detected using AFLP methods. *J. Am. Soc. Hort. Sci.* **2004**, *129*, 559–569. [CrossRef]
4. Montaño, A.; Beato, V.M.; Mansilla, F.; Orgaz, F. Effect of genetic characteristics and environmental factors on organosulfur compounds in garlic (*Allium sativum* L.) grown in Andalusia, Spain. *J. Agric. Food. Chem.* **2011**, *59*, 1301–1307. [CrossRef] [PubMed]
5. Volk, G.M. Phenotypic characteristics of ten garlic cultivars grown at different North American locations. *Hort. Sci.* **2009**, *44*, 1238–1247. [CrossRef]
6. Wang, H.; Li, X.; Shen, D.; Oiu, Y.; Song, J. Diversity evaluation of morphological traits and allicin content in garlic (*Allium sativum* L.) from China. *Euphytica* **2014**, *198*, 243–254. [CrossRef]
7. Leite, V.S.A.; Reis, M.R.; Pinto, F.G. Untargeted metabolomics reveals metabolic changes linked to bulb purpling in garlic (*Allium sativum* L.). *ACS Food Sci. Technol.* **2021**, *1*, 242–248. [CrossRef]
8. Lanzotti, V. Bioactive polar natural compounds from garlic and onions. *Phytochem. Rev.* **2012**, *11*, 179–196. [CrossRef]
9. Lawson, L.D. Bioactive organosulfur compounds of garlic and garlic products. In *Human Medicinal Agents from Plants*; ACS Symposium Series; American Chemical Society: Washington, DC, USA, 1993; Volume 534, pp. 306–330.
10. Block, E. The organosulfur chemistry of the genus *Allium*. Implications for the organic chemistry of sulfur. *Angew. Chem.* **1992**, *31*, 1135–1178. [CrossRef]
11. Lawson, L.D. Garlic: A review of its medicinal effects and indicated active compounds. In *Phytomedicines of Europe*; ACS Symposium Series; American Chemical Society: Washington, DC, USA, 1998; Volume 691, pp. 176–209.
12. Abdelrahman, M.; Hirata, S.; Mukae, T.; Yamada, T.; Sawada, Y.; El-Syaed, M.; Yamada, Y.; Sato, M.; Hirai, M.Y.; Shigyo, M. Comprehensive metabolite profiling in genetic resources of garlic (*Allium sativum* L.) collected from different geographical regions. *Molecules* **2021**, *26*, 1415. [CrossRef]
13. Molino, R.; Rellin, K.F.B.; Nellas, R.B.; Junio, H.A. Small in size, big on taste: Metabolomics analysis of flavor compounds from Philippine garlic. *PLoS ONE* **2021**, *16*, e0247289. [CrossRef] [PubMed]
14. Liu, P.; Weng, R.; Sheng, X.; Wang, X.; Zhang, W.; Qian, Y.; Qiu, J. Profiling of organosulfur compounds and amino acids in garlic from different regions of China. *Food Chem.* **2020**, *305*, 125499. [CrossRef] [PubMed]
15. Hirata, S.; Abdelrahman, M.; Yamauchi, N.; Shigyo, M. Characteristics of chemical components in genetic resources of garlic *Allium sativum* collected from all over the world. *Genet. Resour. Crop Evol.* **2016**, *63*, 35–45. [CrossRef]
16. Jabbes, N.; Arnault, I.; Auger, J.; Al Mohandes Dridi, B.; Hannachi, C. Agro-morphological markers and organo-sulphur compounds to assess diversity in Tunisian garlic landraces. *Sci. Hortic.* **2012**, *148*, 47–54. [CrossRef]
17. González, R.E.; Soto, V.C.; Sance, M.M.; Camargo, A.B.; Galmarini, C.R. Variability of solids, organosulfur compounds, pungency and health-enhancing traits in garlic (*Allium sativum* L.) cultivars belonging to different ecophysiological groups. *J. Agric. Food. Chem.* **2009**, *57*, 10282–10288. [CrossRef] [PubMed]
18. Kamenetsky, R.; London Shafir, I.; Khassanov, F.; Kik, C.; van Heusden, A.W.; Vrielink-van Ginkel, M.; Burger-Meijer, K.; Auger, J.; Arnault, I.; Rabinowitch, H.D. Diversity in fertility potential and organo-sulphur compounds among garlics from Central Asia. *Biodivers. Conserv.* **2005**, *14*, 281–295. [CrossRef]
19. Sommano, S.; Saratan, N.; Suksathan, R.; Pusadee, T. Chemical composition and comparison of genetic variation of commonly available Thai garlic used as food supplement. *J. Appl. Bot. Food Qual.* **2016**, *89*, 235–242. [CrossRef]

20. Szychowski, K.A.; Rybczyńska-Tkaczyk, K.; Gaweł-Bęben, K.; Świeca, M.; Karaś, M.; Jakubczyk, A.; Matysiak, M.; Binduga, U.E.; Gmiński, J. Characterization of active compounds of different garlic (*Allium sativum* L.) cultivars. *Pol. J. Food Nutr. Sci.* **2018**, *68*, 73–81. [CrossRef]

21. MIPAAF. Aggiornamento Dell'elenco Nazionale dei Prodotti Agroalimentari Tradizionali ai Sensi Dell'articolo 12, Comma 1, della Legge 12 Dicembre 2016, n. 238. (21A01168). Ventunesima Revisione Dell'elenco dei Prodotti Agroalimentari Tradizionali 2021, Serie Generale n.48 del 26-02-2021—Suppl. Ordinario n. 15. Available online: https://www.politicheagricole.it/flex/cm/pages/ServeBLOB.php/L/IT/IDPagina/398 (accessed on 20 February 2024).

22. Iobbi, V.; Santoro, V.; Maggi, N.; Giacomini, M.; Lanteri, A.P.; Minuto, G.; Minuto, A.; Fossa, P.; De Tommasi, N.; Bisio, A.; et al. Characterization of sulfur compounds and antiviral activity against *Tomato brown rugose fruit* virus (ToBRFV) of Italian "Vessalico" garlic compared to other cultivars and landrace. *LWT* **2023**, *174*, 114411. [CrossRef]

23. GEVES. *Le Catalogue Officiel des Espèces et Variétés de Plantes Cultivées en France*; GEVES: Beaucouzé, France, 2015.

24. Martins, N.; Petropoulos, S.; Ferreira, I.C.F.R. Chemical composition and bioactive compounds of garlic (*Allium sativum* L.) as affected by pre- and post-harvest conditions: A review. *Food Chem.* **2016**, *211*, 41–50. [CrossRef]

25. Ellis, N.; Hattori, C.; Cheema, J.; Donarski, J.; Charlton, A.; Dickinson, M.; Venditti, G.; Kaló, P.; Szabó, Z.; Kiss, G.B.; et al. NMR metabolomics defining genetic variation in pea seed metabolites. *Front. Plant Sci.* **2018**, *9*, 1022. [CrossRef] [PubMed]

26. Bueno, P.C.P.; Lopes, N.P. Metabolomics to characterize adaptive and signaling responses in legume crops under abiotic stresses. *ACS Omega* **2020**, *5*, 1752–1763. [CrossRef] [PubMed]

27. Jo, S.; Song, Y.; Jeong, J.-H.; Hwang, J.; Kim, Y. Geographical discrimination of *Allium* species (garlic and onion) using 1H NMR spectroscopy with multivariate analysis. *Int. J. Food Prop.* **2020**, *23*, 241–254. [CrossRef]

28. Ritota, M.; Casciani, L.; Han, B.-Z.; Cozzolino, S.; Leita, L.; Sequi, P.; Valentini, M. Traceability of Italian garlic (*Allium sativum* L.) by means of HRMAS-NMR spectroscopy and multivariate data analysis. *Food Chem.* **2012**, *135*, 684–693. [CrossRef] [PubMed]

29. Pacholczyk-Sienicka, B.; Modranka, J.; Ciepielowski, G. Comparative analysis of bioactive compounds in garlic owing to the cultivar and origin. *Food Chem.* **2024**, *439*, 138141. [CrossRef] [PubMed]

30. Muhie, S.H. Novel approaches and practices to sustainable agriculture. *J. Agric. Food Res.* **2022**, *10*, 100446. [CrossRef]

31. Fenibo, E.O.; Ijoma, G.N.; Matambo, T. Biopesticides in sustainable agriculture: A critical sustainable development driver governed by green chemistry principles. *Front. Sustain. Food Syst.* **2021**, *5*, 619058. [CrossRef]

32. Singh, S.; Kumar, V.; Datta, S.; Dhanjal, D.S.; Singh, J. Plant disease management by bioactive natural products. In *Natural Bioactive Products in Sustainable Agriculture*; Singh, J., Yadav, A.N., Eds.; Springer: Singapore, 2020; pp. 15–29.

33. Iqbal, A.; Hamayun, M.; Shah, F.; Hussain, A. Role of plant bioactives in sustainable agriculture. In *Environment, Climate, Plant and Vegetation Growth*; Fahad, S., Hasanuzzaman, M., Alam, M., Ullah, H., Saeed, M., Ali Khan, I., Adnan, M., Eds.; Springer International Publishing: Cham, Switzerland, 2020; pp. 591–605.

34. Vicente, J.G.; Holub, E.B. *Xanthomonas campestris* pv. *campestris* (cause of black rot of crucifers) in the genomic era is still a worldwide threat to brassica crops. *Mol. Plant Pathol.* **2013**, *14*, 2–18. [CrossRef]

35. Gazdik, F.; Magnus, S.; Roberts, S.J.; Baranski, R.; Cechova, J.; Pokluda, R.; Eichmeier, A.; Grzebelus, D.; Baranek, M. Persistence of *Xanthomonas campestris* pv. *campestris* in field soil in Central Europe. *Microorganisms* **2021**, *9*, 591. [CrossRef] [PubMed]

36. Shigaki, T.; Nelson, S.C.; Alvarez, A.M. Symptomless spread of blight-inducing strains of *Xanthomonas campestris* pv. *campestris* on cabbage seedlings in misted seedbeds. *Eur. J. Plant Pathol.* **2000**, *106*, 339–346. [CrossRef]

37. Siddiqui, N.; Mothana, R.; Alam, P. Quantitative determination of alliin in dried garlic cloves and products by high-performance thin-layer chromatography. *Trop. J. Pharm. Res.* **2016**, *15*, 1759. [CrossRef]

38. EPPO. Guidelines on good plant protection practice—Vegetable brassicas. *EPPO Bull.* **1996**, *26*, 311–347.

39. Hakalová, E.; Čechová, J.; Tekielska, D.A.; Eichmeier, A.; Pothier, J.F. Combined effect of thyme and clove phenolic compounds on *Xanthomonas campestris* pv. *campestris* and biocontrol of black rot disease on cabbage seeds. *Front. Microbiol.* **2022**, *13*, 1007988. [CrossRef] [PubMed]

40. Fontana, R.; Caproni, A.; Sicurella, M.; Manfredini, S.; Baldisserotto, A.; Marconi, P. Effects of flavonoids and phenols from *Moringa oleifera* leaf extracts on biofilm processes in *Xanthomonas campestris* pv. *campestris*. *Plants* **2023**, *12*, 1508. [CrossRef] [PubMed]

41. Velasco, P.; Lema, M.; Francisco, M.; Soengas, P.; Cartea, M.E. In vivo and in vitro effects of secondary metabolites against *Xanthomonas campestris* pv. *campestris*. *Molecules* **2013**, *18*, 11131–11143. [CrossRef] [PubMed]

42. da Silva, R.S.; de Oliveira, M.M.G.; de Melo, J.O.; Blank, A.F.; Corrêa, C.B.; Scher, R.; Fernandes, R.P.M. Antimicrobial activity of *Lippia gracilis* essential oils on the plant pathogen *Xanthomonas campestris* pv. *campestris* and their effect on membrane integrity. *Pestic. Biochem. Physiol.* **2019**, *160*, 40–48. [CrossRef] [PubMed]

43. Ali, M.; Ahmad, H.; Hayat, S.; Ghani, M.I.; Amin, B.; Atif, M.J.; Wali, K.; Cheng, Z. Application of garlic allelochemicals improves growth and induces defense responses in eggplant (*Solanum melongena*) against *Verticillium dahliae*. *Ecotoxicol. Environ. Saf.* **2021**, *215*, 112132. [CrossRef] [PubMed]

44. Hayat, S.; Ahmad, H.; Ali, M.; Hayat, K.; Khan, M.A.; Cheng, Z. Aqueous garlic extract as a plant biostimulant enhances physiology, improves crop quality and metabolite abundance, and primes the defense responses of receiver plants. *Appl. Sci.* **2018**, *8*, 1505. [CrossRef]

45. Curtis, H.; Noll, U.; Störmann, J.; Slusarenko, A. Broad-spectrum activity of the volatile phytoanticipin allicin in extracts of garlic (*Allium sativum* L.) against plant pathogenic bacteria, fungi and Oomycetes. *Physiol. Mol. Plant Pathol.* **2004**, *65*, 79–89. [CrossRef]

46. European Commission. *Commission Regulation (EC) No 889/2008 of 5 September 2008—Laying Down Detailed Rules for the Implementation of Council Regulation (EC) No 834/2007 on Organic Production and Labelling of Organic Products with Regard to Organic Production, Labelling and Control*; Document 32008R0889; European Commission: Brussels, Belgium, 2008.

47. European Commission. *Commission Implementing Regulation (EU) 2018/1584 of 22 October 2018—Amending Regulation (EC) No 889/2008 Laying Down Detailed Rules for the Implementation of Council Regulation (EC) No 834/2007 on Organic Production and Labelling of Organic Products with Regard to Organic Production, Labelling and Control*; Implementing Regulation (EU) 2018/1584; European Commission: Brussels, Belgium, 2018.

48. European Commission. *Commission Implementing Regulation (EU) 2021/129 of 3 February 2021—Renewing the Approval of the Active Substance Garlic Extract in Accordance with Regulation (EC) No 1107/2009 of the European Parliament and of the Council Concerning the Placing of Plant Protection Products on the Market, and Amending the Annex to Commission Implementing Regulation (EU) No 540/2011 (Text with EEA Relevance)*; Document 32021R0129, Implementing Regulation (EU) 2021/129; European Commission: Brussels, Belgium, 2021.

49. European Parliament. *Directive 2009/128/EC of the European Parliament and of the Council of 21 October 2009 Establishing a Framework for Community Action to Achieve the Sustainable Use of Pesticides*; European Parliament: Strasbourg, France, 2009; pp. 71–84.

50. European Parliament Council of the European Union. *Regulation (EC) No 1107/2009 of the European Parliament and of the Council of 21 October 2009—Concerning the Placing of Plant Protection Products on the Market and Repealing Council Directives 79/117/EEC and 91/414/EEC*; Document 32009R1107, Regulation (EC) No 1107/2009; European Parliament Council of the European Union: Brussels, Belgium, 2009.

51. Liang, T.; Wei, F.; Lu, Y.; Kodani, Y.; Nakada, M.; Miyakawa, T.; Tanokura, M. Comprehensive NMR Analysis of Compositional Changes of Black Garlic during Thermal Processing. *J. Agric. Food. Chem.* **2015**, *63*, 683–691. [CrossRef]

52. Davies, D.L.; Bouldin, D.W. A cluster separation measure. *IEEE Trans. Pattern Anal. Mach. Intell.* **1979**, *1*, 224–227. [CrossRef] [PubMed]

53. Cameron, A.; Sarojini, V. *Pseudomonas syringae* pv. actinidiae: Chemical control, resistance mechanisms and possible alternatives. *Plant Pathol.* **2014**, *63*, 1–11. [CrossRef]

54. Németh, J. Practice of applying streptomycin to control fireblight in Hungary. In Proceedings of the EPPO Conference on Fireblight, Budapest, Hungary, 7–9 October 2003; EPPO: Paris, France, 2004; pp. 381–382.

55. Verhaegen, M.; Bergot, T.; Liebana, E.; Stancanelli, G.; Streissl, F.; Mingeot-Leclercq, M.-P.; Mahillon, J.; Bragard, C. On the use of antibiotics to control plant pathogenic bacteria: A genetic and genomic perspective. *Front. Microbiol.* **2023**, *14*, 1221478. [CrossRef] [PubMed]

56. Miller, S.A.; Ferreira, J.P.; LeJeune, J.T. Antimicrobial use and resistance in plant agriculture: A one health perspective. *Agriculture* **2022**, *12*, 289. [CrossRef]

57. Pirela, M.; Peña, M.; Peña-Vera, M.; Sulbarán, M.; Perez, E.; Lárez Velásquez, C. Characterization and determination of antimicrobial and metal resistant profiles of *Xanthomonas* strains isolated from natural environments. *J. Anal. Pharm. Res.* **2019**, *8*, 55–60. [CrossRef]

58. Srivastava, V.; Deblais, L.; Kathayat, D.; Rotondo, F.; Helmy, Y.A.; Miller, S.A.; Rajashekara, G. Novel small molecule growth inhibitors of *Xanthomonas* spp. causing bacterial spot of tomato. *Phytopathology* **2021**, *111*, 940–953. [CrossRef] [PubMed]

59. Block, E. The chemistry of garlic and onions. *Sci. Am.* **1985**, *252*, 114–119. [CrossRef] [PubMed]

60. Amagase, H. Clarifying the real bioactive constituents of garlic. *J. Nutr.* **2006**, *136*, 716s–725s. [CrossRef] [PubMed]

61. Ichikawa, M.; Ide, N.; Ono, K. Changes in organosulfur compounds in garlic cloves during storage. *J. Agric. Food. Chem.* **2006**, *54*, 4849–4854. [CrossRef]

62. Beato, V.M.; Sánchez, A.H.; de Castro, A.; Montaño, A. Effect of processing and storage time on the contents of organosulfur compounds in pickled blanched garlic. *J. Agric. Food. Chem.* **2012**, *60*, 3485–3491. [CrossRef]

63. Hornickova, J.; Kubec, R.; Cejpek, K.; Velisek, J.; Ovesna, J.; Stavelikova, H. Profiles of *S*-alk(en)ylcysteine sulfoxides in various garlic genotypes. *Czech J. Food Sci.* **2010**, *28*, 298–308. [CrossRef]

64. Kodera, Y.; Kurita, M.; Nakamoto, M.; Matsutomo, T. Chemistry of aged garlic: Diversity of constituents in aged garlic extract and their production mechanisms via the combination of chemical and enzymatic reactions (Review). *Exp. Ther. Med.* **2020**, *19*, 1574–1584. [CrossRef] [PubMed]

65. Montaño, A.; Casado, F.J.; de Castro, A.; Sánchez, A.H.; Rejano, L. Vitamin content and amino acid composition of pickled garlic processed with and without fermentation. *J. Agric. Food. Chem.* **2004**, *52*, 7324–7330. [CrossRef] [PubMed]

66. Liu, J.; Liu, L.; Guo, W.; Fu, M.; Yang, M.; Huang, S.; Zhang, F.; Liu, Y. A new methodology for sensory quality assessment of garlic based on metabolomics and an artificial neural network. *RSC Adv.* **2019**, *9*, 17754–17765. [CrossRef] [PubMed]

67. Molina-Calle, M.; de Medina, V.S.; Priego-Capote, F.; de Castro, M.D.L. Establishing compositional differences between fresh and black garlic by a metabolomics approach based on LC–QTOF MS/MS analysis. *J. Food Compos. Anal.* **2017**, *62*, 155–163. [CrossRef]

68. Hrbek, V.; Rektorisova, M.; Chmelarova, H.; Ovesna, J.; Hajslova, J. Authenticity assessment of garlic using a metabolomic approach based on high resolution mass spectrometry. *J. Food Compos. Anal.* **2018**, *67*, 19–28. [CrossRef]

69. Chen, Z.; Xu, M.; Wang, C.; Zhou, H.; Fan, L.; Huang, X. Thermolysis kinetics and thermal degradation compounds of alliin. *Food Chem.* **2017**, *223*, 25–30. [CrossRef] [PubMed]

70. Zaini, A.S.; Putra, N.R.; Idham, Z.; Mohd Faizal, A.N.; Che Yunus, M.A.; Mamat, H.; Abdul Aziz, A.H. Comparison of alliin recovery from *Allium sativum* L. using soxhlet extraction and subcritical water extraction. *Chem. Eng.* **2022**, *6*, 73. [CrossRef]

71. Bloem, E.; Haneklaus, S.; Schnug, E. Storage life of field-grown garlic bulbs (*Allium sativum* L.) as influenced by nitrogen and sulfur fertilization. *J. Agric. Food Chem.* **2011**, *59*, 4442–4447. [CrossRef]
72. Lawson, L.D.; Wood, S.G.; Hughes, B.G. HPLC analysis of allicin and other thiosulfinates in garlic clove homogenates. *Planta Med.* **1991**, *57*, 263–270. [CrossRef]
73. Fujisawa, H.; Suma, K.; Origuchi, K.; Kumagai, H.; Seki, T.; Ariga, T. Biological and chemical stability of garlic-derived allicin. *J. Agric. Food. Chem.* **2008**, *56*, 4229–4235. [CrossRef] [PubMed]
74. Rybak, M.E.; Calvey, E.M.; Harnly, J.M. Quantitative determination of allicin in garlic: supercritical fluid extraction and standard addition of alliin. *J. Agric. Food. Chem.* **2004**, *52*, 682–687. [CrossRef] [PubMed]
75. Kodera, Y.; Suzuki, A.; Imada, O.; Kasuga, S.; Sumioka, I.; Kanezawa, A.; Taru, N.; Fujikawa, M.; Nagae, S.; Masamoto, K.; et al. Physical, chemical, and biological properties of *S*-allylcysteine, an amino acid derived from garlic. *J. Agric. Food. Chem.* **2002**, *50*, 622–632. [CrossRef]
76. Rais, N.; Ved, A.; Ahmad, R.; Kumar, M.; Deepak Barbhai, M.; Radha; Chandran, D.; Dey, A.; Dhumal, S.; Senapathy, M.; et al. *S*-Allyl-L-Cysteine—A garlic bioactive: Physicochemical nature, mechanism, pharmacokinetics, and health promoting activities. *J. Funct. Foods* **2023**, *107*, 105657. [CrossRef]
77. Bae, S.E.; Cho, S.Y.; Won, Y.D.; Lee, S.H.; Park, H.J. A comparative study of the different analytical methods for analysis of *S*-allyl-cysteine in black garlic by HPLC. *LWT* **2012**, *46*, 532–535. [CrossRef]
78. Yudhistira, B.; Punthi, F.; Lin, J.-A.; Sulaimana, A.S.; Chang, C.-K.; Hsieh, C.-W. *S*-Allyl cysteine in garlic (*Allium sativum*): Formation, biofunction, and resistance to food processing for value-added product development. *Compr. Rev. Food Sci. Food Saf.* **2022**, *21*, 2665–2687. [CrossRef]
79. Park, S.H.; Lee, H.; Kim, H.S.; Kim, Y.-R.; Noh, S.H. Optimum conditions for *S*-allyl-(L)-cysteine accumulation in aged garlic by RSM. *Food Sci. Biotechnol.* **2014**, *23*, 717–722. [CrossRef]
80. Bae, S.E.; Cho, S.Y.; Won, Y.D.; Lee, S.H.; Park, H.J. Changes in *S*-allyl cysteine contents and physicochemical properties of black garlic during heat treatment. *LWT* **2014**, *55*, 397–402. [CrossRef]
81. Le Mao, I.; Martin-Pernier, J.; Bautista, C.; Lacampagne, S.; Richard, T.; Da Costa, G. ^{1}H-NMR Metabolomics as a tool for winemaking monitoring. *Molecules* **2021**, *26*, 6771. [CrossRef]
82. Wang, K.; Liao, X.; Xia, J.; Xiao, C.; Deng, J.; Xu, Z. Metabolomics: A promising technique for uncovering quality-attribute of fresh and processed fruits and vegetables. *Trends Food Sci. Technol.* **2023**, *142*, 104213. [CrossRef]
83. Salgotra, R.K.; Chauhan, B.S. Genetic diversity, conservation, and utilization of plant genetic resources. *Genes* **2023**, *14*, 174. [CrossRef] [PubMed]
84. Azizi, M.M.F.; Lau, H.Y.; Abu-Bakar, N. Integration of advanced technologies for plant variety and cultivar identification. *J. Biosci.* **2021**, *46*, 91. [CrossRef]
85. Lazaridi, E.; Kapazoglou, A.; Gerakari, M.; Kleftogianni, K.; Passa, K.; Sarri, E.; Papasotiropoulos, V.; Tani, E.; Bebeli, P.J. Crop landraces and indigenous varieties: A valuable source of genes for plant breeding. *Plants* **2024**, *13*, 758. [CrossRef] [PubMed]
86. Jamali, S.H.; Cockram, J.; Hickey, L.T. Insights into deployment of DNA markers in plant variety protection and registration. *Theor. Appl. Genet.* **2019**, *132*, 1911–1929. [CrossRef]
87. Reddy, P.P. *Agro-Ecological Approaches to Pest Management for Sustainable Agriculture*; Springer Nature: Singapore, 2017; p. 339.
88. European Food Safety Authority. The 2017 European Union Report on Pesticide Residues in Food. *EFSA J.* **2019**, *17*, e05743.
89. Directorate-General for Health and Food Safety. *Pesticides*; SANTE: Brussel, Belgium, 2023.
90. Godlewska, K.; Ronga, D.; Michalak, I. Plant extracts—Importance in sustainable agriculture. *Ital. J. Agron.* **2021**, *16*, 1851. [CrossRef]
91. Hayat, S.; Ahmad, A.; Ahmad, H.; Hayat, K.; Khan, M.A.; Runan, T. Garlic, from medicinal herb to possible plant bioprotectant: A review. *Sci. Hortic.* **2022**, *304*, 111296. [CrossRef]
92. La Torre, A.; Iovino, V.; Caradonia, F. Copper in plant protection: Current situation and prospects. *Phytopathol. Mediterr.* **2018**, *57*, 201–236. [CrossRef]
93. Tamm, L.; Thuerig, B.; Apostolov, S.; Blogg, H.; Borgo, E.; Corneo, P.E.; Fittje, S.; de Palma, M.; Donko, A.; Experton, C.; et al. Use of copper-based fungicides in organic agriculture in twelve European countries. *Agronomy* **2022**, *12*, 673. [CrossRef]
94. Bonn, W.G.; Lesage, S. Control of bacterial speck of tomato by copper and ethylenebisuithiocarbamate fungicides: Their efficacy and residues on leaves. *J. Environ. Sci. Health Part B Pestic. Food Contam. Agric. Wastes* **1984**, *19*, 29–38. [CrossRef]
95. Roberts, J.M.; Bruce, T.J.A.; Monaghan, J.M.; Pope, T.W.; Leather, S.R.; Beacham, A.M. Vertical farming systems bring new considerations for pest and disease management. *Ann. Appl. Biol.* **2020**, *176*, 226–232. [CrossRef]
96. Fontana, R.; Caproni, A.; Buzzi, R.; Sicurella, M.; Buratto, M.; Salvatori, F.; Pappadà, M.; Manfredini, S.; Baldisserotto, A.; Marconi, P. Effects of *Moringa oleifera* leaf extracts on *Xanthomonas campestris* pv. *campestris*. *Microorganisms* **2021**, *9*, 2244. [CrossRef] [PubMed]
97. Darji, B.; Ratani, J.; Doshi, M.; Kothari, V. In vitro antimicrobial activity in certain plant products / seed extracts against selected phytopathogens. *Res. Pharm.* **2012**, *2*, 1–10.
98. Guimarães, P.; Moreira, I.; Pedro Campos, P.; Ferraz, J.; Novaes, Q.; Batista, R. Antibacterial activity of *Schinopsis brasiliensis* against phytopathogens of agricultural interest. *Rev. Fitos* **2015**, *9*, 161–252. [CrossRef]
99. Choo, S.; Chin, V.K.; Wong, E.H.; Madhavan, P.; Tay, S.T.; Yong, P.V.C.; Chong, P.P. Review: Antimicrobial properties of allicin used alone or in combination with other medications. *Folia Microbiol.* **2020**, *65*, 451–465. [CrossRef] [PubMed]

100. Khameneh, B.; Iranshahy, M.; Soheili, V.; Fazly Bazzaz, B.S. Review on plant antimicrobials: A mechanistic viewpoint. *Antimicrob. Resist. Infect. Control* **2019**, *8*, 118. [CrossRef] [PubMed]

101. Bloem, E.; Haneklaus, S.; Schnug, E. Influence of fertilizer practices on *S*-containing metabolites in garlic (*Allium sativum* L.) under field conditions. *J. Agric. Food. Chem.* **2010**, *58*, 10690–10696. [CrossRef] [PubMed]

102. Chen, C.; Liu, C.-H.; Cai, J.; Zhang, W.; Qi, W.-L.; Wang, Z.; Liu, Z.-B.; Yang, Y. Broad-spectrum antimicrobial activity, chemical composition and mechanism of action of garlic (*Allium sativum*) extracts. *Food Control* **2018**, *86*, 117–125. [CrossRef]

103. Varympopi, A.; Dimopoulou, A.; Papafotis, D.; Avramidis, P.; Sarris, I.; Karamanidou, T.; Kerou, A.K.; Vlachou, A.; Vellis, E.; Giannopoulos, A.; et al. Antibacterial activity of copper nanoparticles against *Xanthomonas campestris* pv. *vesicatoria* in tomato plants. *Int. J. Mol. Sci.* **2022**, *23*, 4080. [CrossRef]

104. Fan, Q.; Liao, Y.-Y.; Kunwar, S.; Da Silva, S.; Young, M.; Santra, S.; Minsavage, G.V.; Freeman, J.H.; Jones, J.B.; Paret, M.L. Antibacterial effect of copper composites against *Xanthomonas euvesicatoria*. *Crop Prot.* **2021**, *139*, 105366. [CrossRef]

105. Kim, J.-S.; Kim, K.-M.; Kang, S.-W.; Kim, J.-Y.; Kim, J.-Y.; Kim, J.-H. Synergistic antibacterial effect of geraniol, thymol and o-vanillin against *Xanthomonas campestris* pv. *vesicatoria*. *Korean J. Pestic. Sci.* **2023**, *27*, 318–323. [CrossRef]

106. Hanelt, P. Taxonomy, evolution, and history. In *Onions and Allied Crops*; Brewster, J.L., Rabinowitch, H.D., Eds.; CRC Press: Boca Raton, FL, USA, 1989; Volume I: Botany Physiology and Genetics, pp. 1–26.

107. Takagi, H. Garlic (*Allium sativum*). In *Onions and Allied Crops*; Brewster, J.L., Rabinowitch, H.D., Eds.; CRC Press, Taylor & Francis Group: Boca Raton, FL, USA, 2019; Volume III: Biochemistry, Food Science, and Minor Crops, pp. 109–146.

108. Tajidin, N.E.; Shaari, K.; Maulidiani, M.; Salleh, N.S.; Ketaren, B.R.; Mohamad, M. Metabolite profiling of *Andrographis paniculata* (Burm. f.) Nees. young and mature leaves at different harvest ages using ^{1}H NMR-based metabolomics approach. *Sci. Rep.* **2019**, *9*, 16766. [CrossRef] [PubMed]

109. Wang, H.; Li, X.; Liu, X.; Shen, D.; Qiu, Y.; Zhang, X.; Song, J. Influence of pH, concentration and light on stability of allicin in garlic (*Allium sativum* L.) aqueous extract as measured by UPLC. *J. Sci. Food Agric.* **2015**, *95*, 1838–1844. [CrossRef]

110. Monzón Daza, G.; Meneses Macías, C.; Forero, A.M.; Rodríguez, J.; Aragón, M.; Jiménez, C.; Ramos, F.A.; Castellanos, L. Identification of α-amylase and α-glucosidase inhibitors and ligularoside A, a new triterpenoid saponin from *Passiflora ligularis* Juss (Sweet Granadilla) leaves, by a nuclear magnetic resonance-based metabolomic study. *J. Agric. Food. Chem.* **2021**, *69*, 2919–2931. [CrossRef] [PubMed]

111. Vignoli, A.; Ghini, V.; Meoni, G.; Licari, C.; Takis, P.G.; Tenori, L.; Turano, P.; Luchinat, C. High-throughput metabolomics by ^{1}D NMR. *Angew. Chem.* **2019**, *58*, 968–994. [CrossRef] [PubMed]

112. Iobbi, V.; Donadio, G.; Lanteri, A.P.; Maggi, N.; Kirchmair, J.; Parisi, V.; Minuto, G.; Copetta, A.; Giacomini, M.; Bisio, A.; et al. Targeted metabolite profiling of *Salvia rosmarinus* Italian local ecotypes and cultivars and inhibitory activity against *Pectobacterium carotovorum* subsp. *carotovorum*. *Front. Plant Sci.* **2024**, *15*, 1164859. [CrossRef] [PubMed]

113. Lanzotti, V. The analysis of onion and garlic. *J. Chromatogr. A* **2006**, *1112*, 3–22. [CrossRef] [PubMed]

114. Lucas-Torres, C.; Huber, G.; Ichikawa, A.; Nishiyama, Y.; Wong, A. HR-μMAS NMR-based metabolomics: Localized metabolic profiling of a garlic clove with μg tissues. *Anal. Chem.* **2018**, *90*, 13736–13743. [CrossRef] [PubMed]

115. Sumner, L.W.; Amberg, A.; Barrett, D.; Beale, M.H.; Beger, R.; Daykin, C.A.; Fan, T.W.; Fiehn, O.; Goodacre, R.; Griffin, J.L.; et al. Proposed minimum reporting standards for chemical analysis Chemical Analysis Working Group (CAWG) Metabolomics Standards Initiative (MSI). *Metabolomics* **2007**, *3*, 211–221. [CrossRef]

116. Jacob, D.; Deborde, C.; Lefebvre, M.; Maucourt, M.; Moing, A. NMRProcFlow: A graphical and interactive tool dedicated to 1D spectra processing for NMR-based metabolomics. *Metabolomics* **2017**, *13*, 36. [CrossRef]

117. Grimaldi, M.; Marino, C.; Buonocore, M.; Santoro, A.; Sommella, E.; Merciai, F.; Salviati, E.; De Rosa, A.; Nuzzo, T.; Errico, F.; et al. Prenatal and early postnatal cerebral D-aspartate depletion influences L-amino acid pathways, bioenergetic processes, and developmental brain metabolism. *J. Proteome Res.* **2021**, *20*, 727–739. [CrossRef] [PubMed]

118. Vatanen, T.; Osmala, M.; Raiko, T.; Lagus, K.; Sysi-Aho, M.; Orešič, M.; Honkela, T.; Lähdesmäki, H. Self-organization and missing values in SOM and GTM. *Neurocomputing* **2015**, *147*, 60–70. [CrossRef]

119. van den Berg, R.A.; Hoefsloot, H.C.; Westerhuis, J.A.; Smilde, A.K.; van der Werf, M.J. Centering, scaling, and transformations: Improving the biological information content of metabolomics data. *BMC Genom.* **2006**, *7*, 142. [CrossRef] [PubMed]

120. Eriksson, L.; Johansson, E.; Kettaneh-Wold, N.; Trygg, J.; Wikström, C.; Wold, S. *Multi- and Megavariate Data Analysis: Part I: Basic Principles and Applications*, 2nd revised and enlarged ed.; Umetrics Umeå: Umeå, Sweden, 2006.

121. Triba, M.N.; Le Moyec, L.; Amathieu, R.; Goossens, C.; Bouchemal, N.; Nahon, P.; Rutledge, D.N.; Savarin, P. PLS/OPLS models in metabolomics: The impact of permutation of dataset rows on the K-fold cross-validation quality parameters. *Mol. Biosyst.* **2015**, *11*, 13–19. [CrossRef] [PubMed]

122. Agrios, G.N. *Plant Pathology*, 5th ed.; Elsevier Academic Press: Amsterdam, The Netherlands, 2005.

123. Ross, L.N.; Woodward, J.F. Koch's postulates: An interventionist perspective. *Stud. Hist. Philos. Biol. Biomed. Sci.* **2016**, *59*, 35–46. [CrossRef] [PubMed]

124. Dogra, D.; Julka, J.M.; Kumar, A. Insight into antimicrobic evaluation techniques and their role in better assessment of antimicrobic agents: A review. *Asian J. Pharm. Clin. Res.* **2021**, *15*, 6–13. [CrossRef]

125. *M07-A9*; Methods for Dilution Antimicrobial Susceptibility Tests for Bacteria That Grow Aerobically. Clinical and Laboratory Standards Institute: Berwyn, PA, USA, 2012.

126. Ankri, S.; Mirelman, D. Antimicrobial properties of allicin from garlic. *Microb. Infect.* **1999**, *1*, 125–129. [CrossRef] [PubMed]

127. Nakamoto, M.; Kunimura, K.; Suzuki, J.I.; Kodera, Y. Antimicrobial properties of hydrophobic compounds in garlic: Allicin, vinyldithiin, ajoene and diallyl polysulfides. *Exp. Ther. Med.* **2020**, *19*, 1550–1553. [CrossRef] [PubMed]

128. Slusarenko, A.J.; Patel, A.; Portz, D. Control of plant diseases by natural products: Allicin from garlic as a case study. *Eur. J. Plant Pathol.* **2008**, *121*, 313–322. [CrossRef]

129. Bal, D.; Kraska-Dziadecka, A.; Gryff-Keller, A. Solution structure of succinylacetone, an unsymmetrical beta-diketone, as studied by 13C NMR and GIAO-DFT calculations. *J. Org. Chem.* **2009**, *74*, 8604–8609. [CrossRef]

130. Bourafai-Aziez, A.; Jacob, D.; Charpentier, G.; Cassin, E.; Rousselot, G.; Moing, A.; Deborde, C. Development, validation, and use of 1H-NMR spectroscopy for evaluating the quality of acerola-based food supplements and quantifying ascorbic acid. *Molecules* **2022**, *27*, 5614. [CrossRef]

131. Fulmer, G.R.; Miller, A.J.M.; Sherden, N.H.; Gottlieb, H.E.; Nudelman, A.; Stoltz, B.M.; Bercaw, J.E.; Goldberg, K.I. NMR chemical shifts of trace impurities: Common laboratory solvents, organics, and gases in deuterated solvents relevant to the organometallic chemist. *Organometallics* **2010**, *29*, 2176–2179. [CrossRef]

132. Gaviglio, C.; Doctorovich, F. Hydrogen-free homogeneous catalytic reduction of olefins in aqueous solutions. *J. Org. Chem.* **2008**, *73*, 5379–5384. [CrossRef] [PubMed]

133. Hibi, M.; Kawashima, T.; Yajima, H.; Smirnov, S.V.; Kodera, T.; Sugiyama, M.; Shimizu, S.; Yokozeki, K.; Ogawa, J. Enzymatic synthesis of chiral amino acid sulfoxides by Fe(II)/α-ketoglutarate-dependent dioxygenase. *Tetrahedron Asymmetry* **2013**, *24*, 990–994. [CrossRef]

134. Higuchi, O.; Tateshita, K.; Nishimura, H. Antioxidative activity of sulfur-containing compounds in *Allium* species for human low-density lipoprotein (ldl) oxidation in vitro. *J. Agric. Food. Chem.* **2003**, *51*, 7208–7214. [CrossRef]

135. Horton, D.; Wałaszek, Z.; Ekiel, I. Conformations of D-gluconic, D-mannonic, and D-galactonic acids in solution, as determined by N.M.R. spectroscopy. *Carbohydr. Res.* **1983**, *119*, 263–268. [CrossRef]

136. Ingallina, C.; Di Matteo, G.; Spano, M.; Acciaro, E.; Campiglia, E.; Mannina, L.; Sobolev, A.P. Byproducts of globe artichoke and cauliflower production as a new source of bioactive compounds in the green economy perspective: An NMR study. *Molecules* **2023**, *28*, 1363. [CrossRef]

137. Jamieson, A.G.; Boutard, N.; Beauregard, K.; Bodas, M.S.; Ong, H.; Quiniou, C.; Chemtob, S.; Lubell, W.D. Positional scanning for peptide secondary structure by systematic solid-phase synthesis of amino lactam peptides. *J. Am. Chem. Soc.* **2009**, *131*, 7917–7927. [CrossRef] [PubMed]

138. Jiménez-Nava, R.A.; Zepeda-Vallejo, L.G.; Santoyo-Tepole, F.; Chávez-Camarillo, G.M.; Cristiani-Urbina, E. RP-HPLC separation and 1H NMR identification of a yellow fluorescent compound—Riboflavin (vitamin B2) produced by the yeast *Hyphopichia wangnamkhiaoensis*. *Biomolecules* **2023**, *13*, 1423. [CrossRef]

139. Kostidis, S.; Addie, R.D.; Morreau, H.; Mayboroda, O.A.; Giera, M. Quantitative NMR analysis of intra- and extracellular metabolism of mammalian cells: A tutorial. *Anal. Chim. Acta* **2017**, *980*, 1–24. [CrossRef]

140. Maldonado, P.D.; Alvarez-Idaboy, J.R.; Aguilar-González, A.; Lira-Rocha, A.; Jung-Cook, H.; Medina-Campos, O.N.; Pedraza-Chaverrí, J.; Galano, A. Role of Allyl group in the hydroxyl and peroxyl radical scavenging activity of s-allylcysteine. *J. Phys. Chem. B* **2011**, *115*, 13408–13417. [CrossRef] [PubMed]

141. Matsuoka, A.; Isogawa, T.; Morioka, Y.; Knappett, B.R.; Wheatley, A.E.H.; Saito, S.; Naka, H. Hydration of nitriles to amides by a chitin-supported ruthenium catalyst. *RSC Adv.* **2015**, *5*, 12152–12160. [CrossRef]

142. Moing, A.; Maucourt, M.; Renaud, C.; Gaudillère, M.; Brouquisse, R.; Lebouteiller, B.; Gousset-Dupont, A.; Vidal, J.; Granot, D.; Denoyes-Rothan, B.; et al. Quantitative metabolic profiling by 1-dimensional 1H-NMR analyses: Application to plant genetics and functional genomics. *Funct. Plant Biol.* **2004**, *31*, 889–902. [CrossRef] [PubMed]

143. Nilsson, M.; Duarte, I.F.; Almeida, C.; Delgadillo, I.; Goodfellow, B.J.; Gil, A.M.; Morris, G.A. High-resolution NMR and diffusion-ordered spectroscopy of port wine. *J. Agric. Food. Chem.* **2004**, *52*, 3736–3743. [CrossRef] [PubMed]

144. Ramos, L.M.; Caldeira, M.M.; Gil, V.M. NMR study of the complexation of D-gulonic acid with tungsten(VI) and molybdenum(VI). *Carbohydr. Res.* **2000**, *329*, 387–397. [CrossRef] [PubMed]

145. Sabino, A.R.; Tavares, S.; Riffel, A.; Li, J.V.; Oliveira, D.J.; Feres, C.; Henrique, L.; Oliveira, J.S.; Correia, G.D.S.; Sabino, A.S.; et al. Short communication 1 H NMR metabolomic approach reveals chlorogenic acid as a response of sugarcane induced by exposure to Diatraea saccharalis. *Ind. Crop. Prod.* **2019**, *140*, 111651. [CrossRef]

146. Verpoorte, R.; Choi, Y.H.; Kim, H.K. NMR-based metabolomics at work in phytochemistry. *Phytochem. Rev.* **2007**, *6*, 3–14. [CrossRef]

147. Wang, M.-C.; Zhang, Q.-J.; Zhao, W.-X.; Wang, X.-D.; Ding, X.; Jing, T.-T.; Song, M.-P. Evaluation of enantiopure N-(ferrocenylmethyl)azetidin-2-yl(diphenyl)methanol for catalytic asymmetric addition of organozinc reagents to aldehydes. *J. Org. Chem.* **2008**, *73*, 168–176. [CrossRef]